THESIS FOR THE DEGREE OF LICENTIATE OF ENGINEERING

Hydrothermal Liquefaction of Kraft Lignin

The influence of capping agents and residence time

ANDERS AHLBOM

Department of Chemistry and Chemical Engineering

CHALMERS UNIVERSITY OF TECHNOLOGY

Gothenburg, Sweden 2021

Hydrothermal Liquefaction of Kraft Lignin
The influence of capping agents and residence time
ANDERS AHLBOM

Thesis for the Degree of Licentiate in Engineering
No: 2021:22

Department of Chemistry and Chemical Engineering
Chalmers University of Technology
SE-412 96 Gothenburg
Sweden
Telephone + 46 (0)31-772 1000

Cover: Picture by Ann Ahlbom Sundqvist.

Printed by Chalmers Reproservice
Gothenburg, Sweden 2021

Hydrothermal Liquefaction of Kraft Lignin

The influence of capping agents and residence time

ANDERS AHLBOM

Department of Chemistry and Chemical Engineering

Chalmers University of Technology

Abstract

In the context of exploring alternatives to replace fossil resources, lignin has been acknowledged as a renewable source of various aromatic compounds that have the potential of being precursors to chemicals as well as fuel additives. Originating from lignocellulosic biomass such as wood, lignin is an amorphous polymer with a high content of aromatic units and, in order to harness these units, it must be depolymerised. A major problem with current depolymerisation techniques, however, is that lignin repolymerises after being depolymerised, and forms an undesirable char fraction. The addition of capping agents and fine-tuning the reaction conditions can be used to mitigate such formation of char.

This work has investigated the depolymerisation of kraft lignin in hydrothermal conditions under varying temperatures (290-335 °C), residence times (1-12 min) and charges of isopropanol (IPA/dry lignin, 0-4.9) which, aside from being a co-solvent, was hypothesised as acting as a capping agent. The influence of these reaction parameters on the molecular weights, yields and elemental compositions of the products was studied, along with changes in the molecular structure compared to the starting lignin.

The product is a suspension of solid material, i.e. char, in an aqueous phase and thus any desired organic liquid phase requires extraction from the aqueous product. While the yield of char increased with temperature and residence time, it decreased with increasing isopropanol loading, suggesting that the isopropanol does in fact act as a capping agent.

Most of the lignin forms a water-soluble fraction that precipitates when the aqueous product phase is acidified, thereby forming the precipitated solids fraction (PS). The components remaining dissolved after acidification of the product phase are known as acid soluble organics (ASO). A portion of the ASO fraction was aromatic monomers, with guaiacol dominating: this result was expected since the lignin was sourced from softwood. The amount of such monomers increased with residence time in the reactor.

Molecular weight analyses showed a rapid depolymerisation of the lignin within 1 min of hydrothermal liquefaction (HTL) treatment via a significant decrease in the molecular weight of all product fractions: char, PS and ASO. Moreover, the carbon-oxygen inter-unit linkages were found to break in this timeframe as well. The repolymerisation reactions started to exceed depolymerisation between residence times of 4 and 12 min, causing the weight average molecular weight (M_w) to increase again. Although minimising the residence time allows the char yield and M_w to be kept low, more monomers were formed at longer residence times. This calls for careful tuning of the residence time in the HTL of kraft lignin.

Keywords: kraft lignin, hydrothermal liquefaction, HTL, isopropanol, residence time

List of publications

This thesis is based on the following appended papers:

Paper I: **Using Isopropanol as a Capping Agent in the Hydrothermal Liquefaction of Kraft Lignin in Near-Critical Water.** Ahlbom A, Maschietti M, Nielsen R, Lyckeskog H, Hasani M, Theliander H. *Energies*. 2021; 14(4):932. https://doi.org/10.3390/en14040932

Paper II: **Towards understanding kraft lignin depolymerisation under hydrothermal conditions** Ahlbom A, Maschietti M, Nielsen R, Hasani M, Theliander H. Accepted for publication in *Holzforschung*.

Contribution report

Paper I: First author. The author planned the experiments together with Hans Theliander, Marco Maschietti and Merima Hasani and performed them with Marco Maschietti and Rudi Nielsen. The author was the main person responsible for the ensuing characterizations, and the results were evaluated in collaboration with the co-authors. The author drafted the manuscript and revised it after receiving co-author feedback.

Paper II: First author. The author planned the experiments together with Hans Theliander, Marco Maschietti and Merima Hasani and performed them with Marco Maschietti and Rudi Nielsen. The author was the main person responsible for the ensuing characterizations, and the results were evaluated in collaboration with the co-authors. The author drafted the manuscript and revised it after receiving co-author feedback.

List of abbreviations

AAS	Atomic Absorption Spectroscopy
ASO	Acid Soluble Organics
ATR	Attenuated Total Reflectance
BHT	Butylated Hydroxytoluene
C-C	Carbon-Carbon bond
CEL	Cellulolytic Enzyme Lignin
CHNS	Elemental analysis of Carbon, Hydrogen, Nitrogen and Sulphur
C-O	Carbon-Oxygen bond
DEE	Diethyl Ether
DMSO	Dimethyl Sulfoxide
DMSO-*d6*	Deuterated Dimethyl Sulfoxide
EMAL	Enzymatic Mild Acidolysis Lignin
EWG	Electron Withdrawing Group
FTIR	Fourier Transform Infrared Spectroscopy
GC	Gas Chromatography
GPC	Gel Permeation Chromatography
HMBC	Heteronuclear Multiple Bond Correlation
HSQC	Heteronuclear Single Quantum Coherence
HTL	Hydrothermal Liquefaction
ICP-OES	Inductively Coupled Plasma - Optical Emission Spectrometry
IPA	Isopropanol
LCC	Lignin Carbohydrate Complex
MS	Mass Spectrometry
M_w	Weight average molecular weight
MWL	Milled Wood Lignin
NMR	Nuclear Magnetic Resonance Spectroscopy

P&I	Piping and Instrumentation
PS	Precipitated Solids
RCF	Reductive Catalytic Fractionation
RI	Refractive Index
THF	Tetrahydrofuran
UV	Ultraviolet Light
WSO	Water Soluble Organics
Xyl	Xylan

Contents

1 Introduction

Interest in the replacement of fossil resources with renewable alternatives is increasing constantly in the light of climate change due to global warming. As resources continue to dwindle, alternatives to fuel and chemicals based on petroleum are necessary, especially from sources that do not directly compete with food production. Lignocellulosic biomass, such as wood and agricultural residues, make plausible candidates to this end. While the cellulosic fraction of these materials has long been used in the production of paper and textiles, for example, the valorisation of the large lignin fraction of lignocellulosic materials remains a challenge. Lignin is an amorphous polymer and represents the largest potential source of renewable aromatics that is readily available (Zakzeski *et al.* 2010). Although it is renowned for its recalcitrance and heterogeneity, which explains its present underutilisation, certain applications nevertheless exist. Methods for harvesting aromatics from lignin could make an important contribution to the replacement of fossil resources considering that, depending on the species and section of the tree, lignin constitutes 15-30 % of wood (Gellerstedt and Henriksson 2008). Furthermore, existing sulphite and kraft pulp mills already remove lignin from wood as an integral part of their process, and methods of extracting this lignin from the pulping cooking liquor already exist. Although lignosulphonates, produced in sulphite pulping, currently have many uses, most lignin is however liberated in kraft pulping mills and incinerated to cover the energy need of these mills. Modern pulp mills with an energy surplus have the potential of extracting

surplus lignin using, for example, the LignoBoost process. Greater amounts of kraft lignin could thus be extracted: in the order of millions of tonnes compared to the current kiloton scale (Dessbesell *et al.* 2020). After depolymerisation, and subsequent separation and aftertreatment, lignin could form fuel additives and chemicals, thereby harnessing its aromatic content. One estimation is that kraft lignin sourced from pulp mills could constitute approx. 2% of the volume of petrochemicals used globally (Berlin and Balakshin 2014).

Depolymerisation may be one first step in the valorisation of extracted lignin. This can be achieved in various ways, for instance by employing pyrolysis, oxidation, reductive techniques and hydrothermal methods. The latter use water at high pressure and temperature to depolymerise the lignin and, by controlling the temperature of the process, the product range of the process can be controlled. Low temperatures favours a solid product, whilst gas can be formed at higher temperatures (Kruse and Dahmen 2015). A temperature level in between provides the possibility of producing a liquid product via hydrothermal liquefaction (HTL), which is appealing as a liquid product makes for easier processing compared to a solid product. A challenge associated with this process, along with other depolymerisation techniques, however, is the tendency of reactive components to repolymerise and form char: this lowers the yield of valuable products and poses operational problems like scaling that forms e.g. in pipes. Not only does the depolymerisation process entail a broad product spectrum calling for an efficient separation, but the operation also needs to be skilfully tuned to reduce repolymerisation. Reaction parameters such as temperature, type of solvent, pH and potential catalyst are important. In addition, residence time in the reactor and additives can also affect the result (Bernhardt *et al.* 2021). Additives can scavenge reactive components during the reactions and prevent repolymerisation: as such, they are known as "capping agents". Boric acid, phenol, methanol and ethanol have all been shown to act as capping agents in reducing the char yield (Arturi *et al.* 2017; Belkheiri *et al.* 2016, 2014; Cheng *et al.* 2012, 2016; Lee *et al.* 2016; Roberts *et al.* 2011; Sebhat 2016). Studies on the use of isopropanol (IPA) are nevertheless scarce, especially in the field of kraft lignin depolymerisation. Furthermore, although there is some evidence of a swift reaction process in the HTL of lignin, the structural changes of the lignin involved at short residence times are not well covered. Consequently, the effects of using IPA as a capping agent in kraft lignin at short residence times remain an open question.

1.1 Aim and scope

The aim of this study is to investigate the efficient depolymerisation of kraft lignin using hydrothermal liquefaction. Aromatic components are thereby liberated, which is part of the larger scope of valorising kraft lignin, and capping agents are added to achieve the suppression of char. Previous work has shown that alcohols such as

methanol and ethanol suppress char formation (possibly by hydrogen transfer) but there is a lack of understanding as to how isopropanol acts as a capping agent in the hydrothermal depolymerisation of kraft lignin.

The first part of the work investigated the effects of adding isopropanol to a hydrothermal liquefaction of kraft lignin in water at subcritical conditions; the effects of reaction temperature were also investigated in the subcritical range. Changes in structure and molecular weight were investigated in order to track the depolymerisation process.

The second part of the work continued to employ isopropanol as a capping agent in the HTL of kraft lignin but focused instead on the residence time in the reactor. Most of the studies carried out on lignin depolymerisation were made in batch reactors with long heating times and, consequently, data on structural changes that occur early on is scarce: attaining a short HTL treatment time is difficult. Studies nonetheless indicate a swift process. Employing a custom-made reactor with an injection system made it possible to reduce the HTL treatment time and to investigate structural changes early in the treatment.

2
Lignin

This chapter opens with the basic chemistry of lignin and its polymerisation. Methods by which lignin can be isolated from biomass are then described.

2.1 Lignocellulosic biomass

Lignocellulosic biomass, such as wood, is comprised of three major constituents: cellulose, hemicellulose and lignin. Cellulose and hemicellulose are carbohydrate polymers, whilst lignin is a polymer built from phenylpropane units. The composition of the polymers present in wood depends on the species of the tree and the section of the wood: typically, the content of cellulose ranges between 40-60 %, lignin 15-30 % and hemicellulose 10-40 % (Schutyser *et al.* 2018). In addition, there are also minor contents of extractives present in the wood (Daniel 2009).

The wood components are ordered on several morphological levels: from small cellulose microfibrils in the cell walls of various types of wood cells, to the composite wood in which various types of wood cells form the stem, roots and branches of the tree. The wood cell walls contain several layers that are composed of cellulose microfibrils oriented in different directions. The varying directions of these microfibrils render strength to the wood structure. Cellulose thus provides a matrix which the lignin and hemicelluloses both support and bind together. In between the wood cells a thin middle lamella, comprised mainly of lignin, serves to glue the wood cells together. Various

types of wood cells, oriented mainly vertically but also radially, are glued together to build the wood structure (Daniel 2009). This composite nature of wood makes it resistant to degradation and provides the strength required for the tree to rise high and stand upright.

2.2 Lignin

After cellulose, lignin constitutes the majority of lignocellulosic biomass such as wood. Lignin is an amorphous polymer, the exact native structure of which remains elusive because it changes during isolation from the biomass. The lignin polymer is synthesised in plant cells from three monolignol units: *p*-coumaryl alcohol, coniferyl alcohol and sinapyl alcohol, as shown in Figure 1. These monolignols are distinguished by the number of methoxy groups attached to the aromatic rings. The sinapyl alcohol contains a syringyl unit, the coniferyl alcohol contains a guaiacyl unit and the *p*-coumaryl alcohol a hydroxy phenol unit and they are therefore referred to as S, G and H, respectively, when incorporated in the lignin structure (Lora 2008).

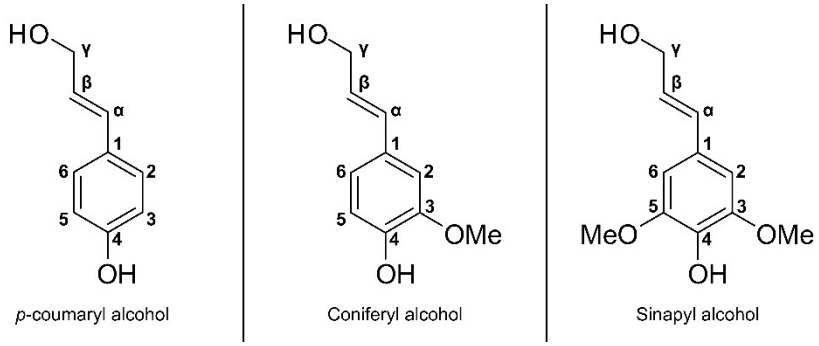

Figure 1: Monolignols present in lignin, with their corresponding nomenclature.

Depending on the species of the plant and the location of the lignin within it, the proportions of these monolignols differ: typically, softwood lignin contains coniferyl alcohol, with small amounts of *p*-coumaryl alcohol and no sinapyl alcohol. Hardwood, on the other hand, contains both sinapyl and coniferyl alcohol (with a ratio ranging from 1 to 3) and might also include some *p*-coumaryl alcohol. Finally, the lignin in grasses contains all three monolignols, with the highest proportion of *p*-coumaryl alcohol of all types of lignin (Henriksson 2009; Lora 2008).

The inter-unit linkages between lignin monomers are labelled according to the nomenclature in Figure 1. The second unit is assigned a prime, as shown in Figure 2, where the common β-O-4' bond is shown with conventional numbering.

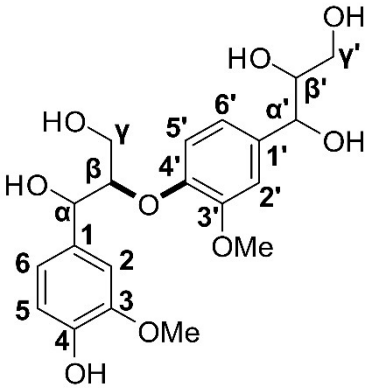

Figure 2: β-O-4' bond with numbering.

Lignin has four primary functions in lignocellulosic biomass: contributing to the stiffness of the cell walls, thus enabling the plants to grow tall; gluing the different cells together in the lignocellulosic tissue; making the cell wall hydrophobic to enable water and nutrient transport in the cells without leakage; and protecting the lignocellulosic tissue from microbial degradation by making the tissue compact and, by virtue of its complex and heterogeneous character, preventing the effective attack of mould (Henriksson 2009). Branching contributes to the gluing function of lignin, thus stiffening the lignocellulosic tissue. Non-covalent dipole interaction of the aromatic groups, along with hydrogen bonding with cellulose and hemicellulose, also contribute to the stiffening of the tissue (Henriksson 2009). Furthermore, lignin-carbohydrate complexes (LCC:s) also form by covalent linkages between carbohydrates and lignin, primarily via phenyl glucoside bonds, benzyl ethers and esters (Berlin and Balakshin 2014). Examples of such LCC complexes are shown in Figure 3.

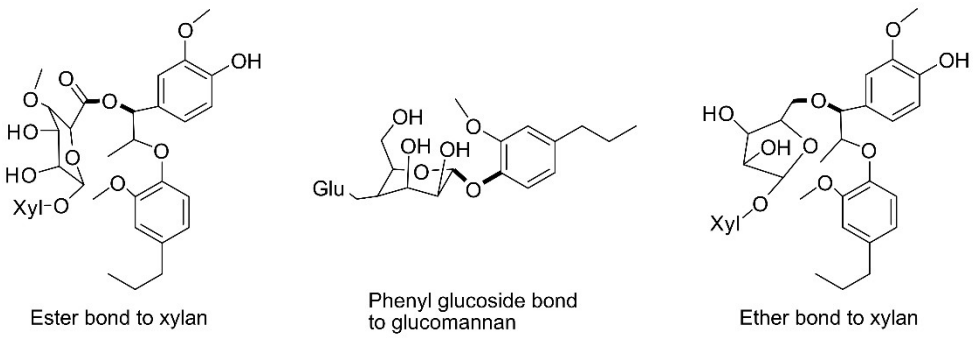

Figure 3: LCC complexes (adapted from Henriksson 2009*). Lignin side chain hydroxyl groups are omitted for clarity.*

2.3 Polymerisation of lignin

Lignin is polymerised by a radical mechanism preceded by oxidation of the phenolic monomers, Figure 1, with either laccase or peroxidase. These enzymes employ oxygen or hydrogen peroxide, respectively, for the oxidation process (Lora 2008). Oxidation targets the phenol group on the monolignols; the radical thus formed is resonance stabilised on positions 4-O, β, 5, 1 and 3, as shown for coniferyl alcohol in Figure 4.

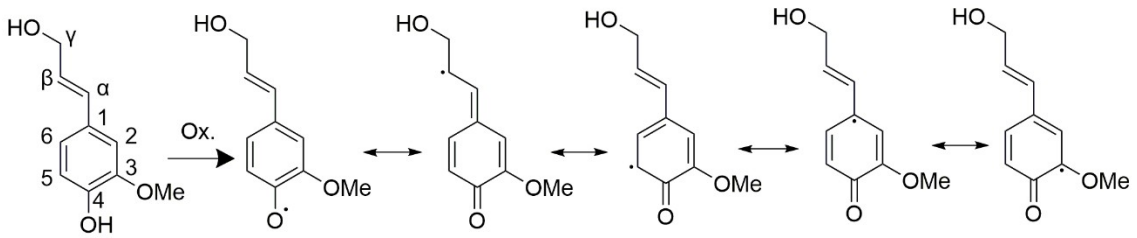

Figure 4: Resonance-stabilised radicals in lignin polymerisation (adapted from Henriksson 2009*).*

It is notable that a quinone methide structure is part of the resonance structure, with the radical on the β position. Reactions between the radicals form the common inter-unit lignin bonds β-O-4', β-5' and β-β', as the unpaired electrons in the radicals form covalent bonds. Subsequent addition of water or intramolecular bonding causes the quinone methide structure to vanish and the well-known lignin linkages to be formed (Henriksson 2009). The formation of β-O-4' is an example of this and is depicted in Figure 5.

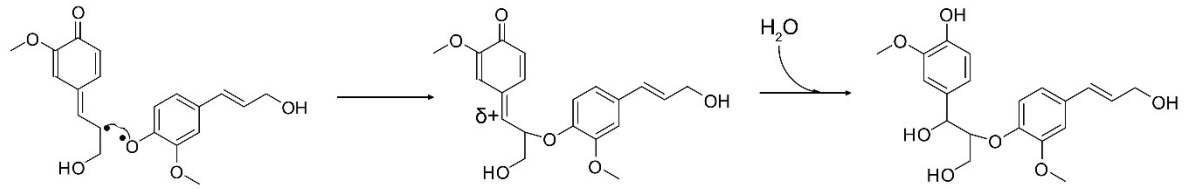

Figure 5: Formation of the β-O-4' bond (adapted from Henriksson 2009*). A carbohydrate may replace the water molecule in the last step and thereby form an LCC complex.*

In the resonance structures of oxidised coniferyl alcohol shown in Figure 4, the C_3 on the coniferyl alcohol is occupied by a methoxy group (-OMe) and therefore does not form inter-unit linkages. If the monolignol is instead sinapyl alcohol, on which both the C_3 and C_5 positions are occupied by methoxy groups, C_5 is also blocked from further reaction, cf. Figure 1. Lignins with sinapyl alcohol (e.g. hardwood lignin) consequently have fewer linkages to the C_5 position, such as β-5' and 5-5'. Softwood lignin is constituted almost exclusively of coniferyl alcohol, shown in Figure 4, with some minor amount *p*-coumaryl alcohol also being present. Thus, bonds such as β-5' and 5-5' are much more common in softwood lignin than in hardwood lignin (Gellerstedt and Henriksson 2008). Hardwood lignin has a larger fraction of β-O-4' bonds and these are weaker than the carbon-carbon (C-C) bonds 5-5' and β-5' (Henriksson 2009; Parthasarathi *et al.* 2011). Typical lignin bonds are presented in Figure 6.

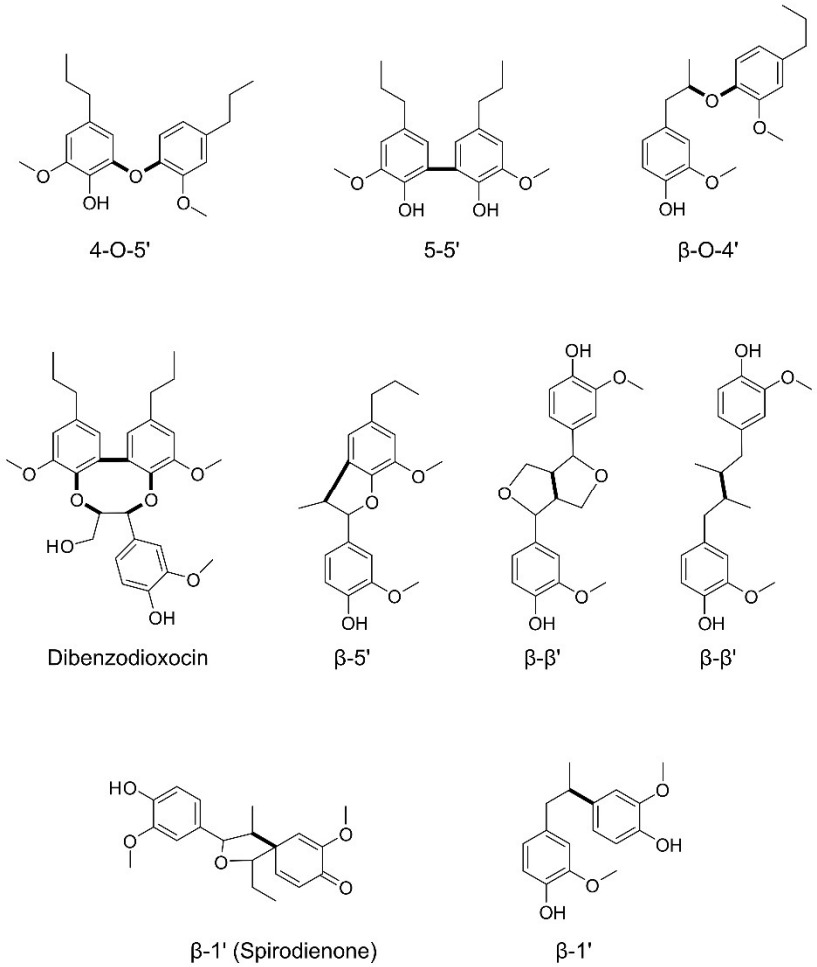

Figure 6: Lignin bonds (adapted from Henriksson 2009). *Propyl side chain hydroxyl groups are omitted for clarity.*

2.4 Isolation of lignin from biomass

Isolating lignin from a lignocellulosic biomass such as wood entails its liberation from the cell walls and middle lamellae. Not only does the lignin need to be degraded and solubilised, but also transported out from both the cell wall and the wood structure. Degradation occurs as lignin bonds are being broken: both the inter-unit linkages in lignin as well as the bonds forming LCCs. The products of these reactions are dissolved in the reaction medium. The dissolved lignin can subsequently be isolated from the reaction medium, e.g. the cooking liquor, either by precipitation and filtration or drying (Gellerstedt *et al.* 2013). This is described further below, in the section "The LignoBoost process".

Depending on the application of the lignin, a varying degree of the structural changes that occur during its isolation can be tolerated. For purposes of research, the aim is often to preserve the lignin structure as close as possible to its native form. One such mild isolation method is ball milling, followed by extraction using a dioxane and water mixture that yields milled wood lignin (MWL). This procedure can be paired with

enzymatic degradation of the residual carbohydrates to form cellulolytic enzyme lignin (CEL) and an additional mild acid hydrolysis to form enzymatic mild acidolysis lignin (EMAL). While these lignins are closest to the native lignin structure and thereby extensively researched, especially in the case of MWL, they are not feasible for use in industrial production processes (Schutyser *et al.* 2018).

Lignin isolated from industrial processes is usually referred to as "technical lignin". Although available in large amounts, technical lignins are not the primary product of the industrial processes extracting them, e.g. pulping. Little consideration of the structure of lignin is therefore taken, since the primary product is paper pulp: lignin is merely a by-product. Larger scale methods for isolating lignin may be grouped based on the conditions employed in the reaction medium, such as acidic and alkaline methods.

2.4.1 Acidic conditions

Acidic methods for isolating lignin from lignocellulosic biomass such as wood include steam explosion, acid hydrolysis with mineral acid addition, acid sulphite pulping and organosolv pulping (Schutyser *et al.* 2018).

Acid hydrolysis targets the carbohydrates in wood, which are decomposed into sugars by adding mineral acids to the reaction: a method used to a large degree in the former Soviet Union in the production of e.g. ethanol for butadiene rubber, xylitol, furfural and fodder yeast (Rabinovich 2010). Both the carbohydrates and lignin are degraded by acid hydrolysis. The benzylic carbon in lignin (C_α in Figure 2) first forms a carbocation; subsequent reactions may break β-O-4' bonds to form Hibbert ketones and thereby degrade the lignin. However, the carbocation may also condense with C_5 and C_6 on aromatic rings, forming strong C-C bonds (Li *et al.* 2007). The acidic methods used to isolate lignin thus may condense it. This condensation can, however, be mitigated if other nucleophiles, such as alcohols or bisulphite ions, are present that can react with the carbocation (Gellerstedt *et al.* 2013). 2-naphtol has also been added successfully as a nucleophile to react with the carbocation in steam explosions (Li *et al.* 2007; Wayman and Lora 1978). Steam explosion involves acidic reactions because acids are released from the wood during the process.

2.4.1.1 Sulphite pulping

Sulphite pulping was once the dominant chemical pulping method employed but has long since been superseded by kraft pulping. While it can be achieved at either acidic, neutral or alkaline conditions, sulphite pulping is most commonly run at acidic conditions (Gellerstedt 2009). Delignification occurs by acid hydrolysis of ether linkages degrading the lignin, along with the incorporation of sulphonate groups into the lignin structure, which also increases the solubility of the lignin in the reaction medium. Bisulphite ions (HSO_3^-) act as nucleophiles and attach to the carbocation on the C_α thereby increasing the polarity and, consequently, the solubility of the lignin in the

pulping liquor. In common with other acidic depolymerisation methods, condensation reactions occur and compete with the sulphonation reaction.

The resulting lignosulphonates are soluble over a wide pH range and are typically not precipitated from the cooking liquor: they are instead isolated through evaporation of the water in the liquor (Gellerstedt *et al.* 2013). It is commonplace that the amount of residual sugars in the spent liquor be reduced by fermentation into ethanol; it is also possible to oxidise parts of the lignosulphonates to produce vanillin, as is the case at the Borregaard Mill in Norway. As such, the sulphite mill can represent a biorefinery with a wide range of products: pulp, ethanol, lignosulphonates and vanillin. Lignosulphonates have an established market as dispersants and binders, with a global annual production of 1.32 Mt (Dessbesell *et al.* 2020).

2.4.1.2 Organosolv pulping

Organosolv pulping involves subjecting the biomass to an organic solvent, such as EtOH, formic acid or acetic acid, at low pH. Such organic components act as nucleophiles and mitigate condensation under acidic conditions, analogously to the bisulphite groups of acidic sulphite pulping (Gellerstedt *et al.* 2013). The degradation of hemicelluloses in the biomass during organosolv pulping produces an acidic environment even without the additional acid, whether mineral or organic. Its more extensive delignification of biomass, caused by the higher solubility of the lignin in the organic solvent compared to a purely aqueous reaction medium, makes the organosolv process more favourable than acid hydrolysis (Schutyser *et al.* 2018). Although not available on an industrial scale as the lignins from conventional pulping processes, e.g. sulphite and kraft pulping, much research has been carried out on Alcell lignin: a type of organosolv lignin produced in a pilot unit by Alcell Technologies Inc. (Dessbesell *et al.* 2020; Thring 1994). Furthermore, research on organosolv lignin often uses lignin isolated by the respective research groups.

2.4.2 Alkaline conditions

Alkaline degradation of lignin occurs in both soda and kraft pulping and, while the active cooking chemical used in both is OH^-, the latter also employs HS^-. The depolymerisation reaction of lignin under alkaline conditions, especially the β-O-4' bond cleavage, is greatly affected by whether the aromatic unit carrying the β-chain is phenolic or not: if it is, then an equilibrium with the corresponding quinone methide forms. Should HS^- be present in the reaction solution, as is the case in kraft pulping, it will attach to the C_α and later form an episulphide with the C_β. The C_β, in turn, expels the oxygen atom of the ether linkage and the β-O-4' is thus cleaved. The quinone methide may instead form enol ether without breaking the β-O-4' if there are no HS^- ions available: this occurs under the expulsion of formaldehyde as the C_γ-C_β bond breaks (Gellerstedt 2009). Other possible reactions are condensation on the C_α or a simple reduction of the C_α to form a methylene unit (Schutyser *et al.* 2018). In alkaline

degradation of β-5' the α-O-4' bond, which is a part of the β-5' bond (cf. Figure 6), breaks when a quinone methide is formed. In the case of the β-5' and β-1' bonds, however, no cleavage of aryl-alkyl C-C linkages can be seen: stilbenes are formed instead as formaldehyde is expelled (Gellerstedt 2009).

Although quinone methide forms only if the aromatic ring is phenolic, the β-O-4' can nevertheless be broken by ionisation of a hydroxyl group on C_α or C_γ. This ionised group attacks the C_β and forms an epoxide ring, causing the β-O in β-O-4' to break. The epoxide may then react with nucleophiles (Gellerstedt 2009): this type of degradation occurs in both soda and kraft pulping. Kraft pulping encompasses the breaking of both phenolic and non-phenolic β-O-4', which makes it more efficient than soda pulping. Together with the high quality of the pulp produced, effective cooking chemical recovery and efficient energy self-sufficiency, this explains its dominance: kraft pulping accounts for 95 % of the current production of chemical pulps (Gellerstedt *et al.* 2013; Schutyser *et al.* 2018). In addition, up to 90-95 % of the lignin in the wood can be removed in the kraft pulping process (Gellerstedt 2015), although repolymerisation and the enrichment of strong C-C bonds, along with a low content of residual β-O-4' bonds, render the kraft lignin recalcitrant to further reactions (Schutyser *et al.* 2018). Furthermore, sulphur is incorporated into the lignin, to an extent of roughly 2-3 % (Gellerstedt *et al.* 2013). Soda pulping, on the other hand, produces lignin devoid of sulphur but its use is limited to producing paper pulp from annual plants such as bagasse, flax, wheat and rice straw (Gellerstedt *et al.* 2013).

Kraft lignin is a very recalcitrant form of lignin. The dominance of kraft pulping, however, combined with efficient and commercial-scale lignin separation techniques, such as the LignoBoost and LignoForce processes, make its investigation relevant; it is also available in abundance. A common estimation, based on a global annual production of 130 Mton of kraft pulp, is that 55 Mt/y of kraft lignin is released into the black liquor of kraft pulping mills (Gellerstedt *et al.* 2013). The absolute majority of this is incinerated in the recovery boilers of the mills for the regeneration of cooking chemicals used in the process and to produce steam to cover their energy demand. A modern mill with an energy surplus can therefore extract lignin and thereby increase pulp production without expanding the recovery boiler (Gellerstedt *et al.* 2013).

2.4.2.1 The LignoBoost process

Kraft lignin is isolated from black liquor by precipitation. There are several commercial processes for achieving this, for instance the LignoBoost and LignoForce processes (Dessbesell *et al.* 2020). The LignoBoost process starts by precipitating lignin from the black liquor obtained after pulping with CO_2 and is followed by filtration in a chamber filter press. Plugging of the filter brought on by ionic strength gradients in the filter cake is avoided by not washing the filter cake in the first filter step, but redispersing it instead. Sulphuric acid is added so that the changes in pH and ionic strength occur

in a slurry tank rather than in the ensuing filter. The slurry is then filtered in a second chamber filter press and washed. The filtrates from the filter steps are recycled to the black liquor evaporator train, and the resulting lignin has a low ash and carbohydrate content (Tomani 2010). An alternative method of kraft lignin extraction is the LignoForce process, which involves the oxidation of black liquor prior to precipitation, filtration and washing (Dessbesell *et al.* 2020).

Removing kraft lignin from black liquor alters the energy balance of the kraft mill in question: unremoved, the lignin would be incinerated and thereby provide energy. In addition, the Na/S balance is affected: salt precipitation, along with changes in the black liquor properties and heating value, must also be considered when removing lignin from black liquor (Gellerstedt 2015). Estimations of the amount of kraft lignin that could be extracted from black liquor globally without compromising the energy balance of the mills vary: from 6-9 Mt/y, representing 6-7 % of the spent liquor, via 3.5-14 Mt/y, representing 5-20 % of the kraft lignin in the mills, and culminating at up to 40 Mt/y, representing 75 % of the lignin processed by kraft pulping mills (Berlin and Balakshin 2014; Björk *et al.* 2015; Dessbesell *et al.* 2020).

2.4.3 *Lignin-first* approaches

In recognition of the important future place that awaits lignin, various attempts that focus on its isolation without causing extensive structural changes, also known as *lignin-first* approaches, continue to gain attraction (Renders *et al.* 2017). Such strategies include mild fractionation to preserve β-O-4' in the lignin, for example by employing mild organosolv conditions or ionic liquid fractionation; extraction in a solvent, coupled with lignin depolymerisation and catalytic hydrogenation with either H_2 or a hydrogen-donating solvent to produce a lignin oil, an approach known as reductive catalytic fractionation (RCF); protecting the β-O-4' linkages by forming acetals with the α-OH and γ-OH groups on the side chain through the addition of formaldehyde, the latter of which also prevents condensation of the aromatic rings by blocking the reactive *meta*-positions, such as C_6 on the aromatic ring (Renders *et al.* 2017; Shuai *et al.* 2016a). These processes shift emphasis from the use of carbohydrates as the main product obtained from biomass and focus on the lignin instead. Nevertheless, until a high value product of the large carbohydrate fraction of the wood in *lignin-first* approaches is established, these processes may be economically unfeasible if the lignin is not valorised substantially enough to cover the cost of the process. While the lignin content can range up to 30%, the majority of the lignocellulosic biomass is in the form of carbohydrates.

2.5 Use of technical lignin

The absolute majority of the present global production of technical lignin, which amounts to 1.65 Mt/y, are lignosulphonates and constitute 80 % of the production (Dessbesell *et al.* 2020). They are used for their surfactant properties, e.g. as bonding agents in pelletisation and dispersants in concrete and ceramics. Vanillin is also produced from lignosulphonates, as mentioned previously. Kraft lignin is produced on a much smaller scale than lignosulphonates, with a capacity of 265 kt/y as of 2018, although this is increasing. Currently, aside from being used as an energy source via combustion, kraft lignin is sulphonated and used as a surfactant, similarly to lignosulphonates (Berlin and Balakshin 2014). Near-term usages of kraft lignin include it replacing phenol in phenol-formaldehyde resins for use in e.g. abrasives and insulation, as well as in engineered wood products such as plywood (Dessbesell *et al.* 2020; Macfarlane *et al.* 2014). Another potential application is as a polyol in the production of polyurethane foams used, for instance, as insulation (Dessbesell *et al.* 2020). More long-term alternatives include it being used in the production of thermoplastics, carbon fibres and liquid fuel applications (Balakshin *et al.* 2021; Castello *et al.* 2018), although these require the lignin to be depolymerised. While the lignosulphonates represent an established market for technical lignin, the production of kraft lignin has increased rapidly over the past years: from a production of 60 kt/y in 2011 to 265 kt/y capacity in 2018 (Dessbesell *et al.* 2020). Considering the dominance of kraft pulping and the estimated production potential of kraft lignin being millions of tonnes, further valorisation of this material is certainly appealing.

3

Lignin Depolymerisation

Isolating lignin from biomass is the first step in its valorisation and in this chapter a brief overview of techniques that can be used for its subsequent depolymerisation is given.

Once lignin has been isolated from biomass, further depolymerisation is a way for its use in production of specialty chemicals or as a fuel additive (Macfarlane *et al.* 2014). While such depolymerisation produces a bio-oil in pyrolysis or bio-crude in hydrothermal liquefaction, their oxygen content might render them unsuitable for direct use. Rather, further treatment is necessary: for instance, by co-feeding the bio-oil or bio-crude into conventional petroleum refineries or by employing hydrotreatment to reduce the oxygen content (Castello and Rosendahl 2018). The depolymerisation of lignin has been a long sought-after goal and can be seen in the broader perspective of the liquefaction of biomass. Castello *et al.* (2018) and Lange (2018) noted that a high oil price correlates well with interest in such bioenergy research. Various methods for depolymerising lignin have been investigated and are described briefly below.

3.1 Hydrotreatment

The chemical structure of lignin resembles low rank coal; its liquefaction was therefore adapted to the Bergius process, a process which was developed during the First World War for the liquefaction of coal with hydrogen. The Noguchi process for lignin

liquefaction was thus developed at the beginning of the 1950s (Nielsen 2016). In the Noguchi process lignin was depolymerised in a reaction mixture of phenols and lignin tars whilst being subjected to hydrogen gas, with iron sulphide as the catalyst and a co-catalyst of another metal sulphide. This process was developed even further, employing various catalysts and feed stocks, by Inventa AG, Universal Oil Products, The Hydrocarbon Research Institute and Shell.

The reaction of lignin with hydrogen may saturate reactive compounds in a hydrogenation process or depolymerise the lignin in a hydrogenolysis process. Moreover, the oxygen content of the lignin may be lowered when using hydrogen in a hydrodeoxygenation process. These different hydrotreatment processes can be tuned by utilising various catalysts. Hydrogenolysis, which depolymerises the lignin, has been investigated with hydrogen in the gas form, typically with solid catalysts, or with liquid hydrogen donating solvents such as tetralin, formic acid or aliphatic alcohols, e.g. ethanol and isopropanol (Huang *et al.* 2015; Kim *et al.* 2014; Kleinert *et al.* 2009; Pandey and Kim 2011).

3.2 Pyrolysis

The technique most investigated for producing lower molecular weight liquids and gaseous products from biomass is pyrolysis, i.e. rapid heating of biomass (such as lignin) in an oxygen-free atmosphere with a very short treatment time, typically in the order of seconds, followed by condensation of the gases thus produced (Pandey and Kim 2011). The raw material, which usually has a low moisture content, is broken down in a thermolytic process (Castello *et al.* 2018). In order to maximise the oil yield from pyrolysis, a high heating rate is paired with a short treatment time of just seconds (Schutyser *et al.* 2018).

Lignin pyrolysis allows weaker bonds to be cleaved at lower temperatures: higher temperatures may cause the aromatic ring to crack (Macfarlane *et al.* 2014). The product of pyrolysis thus contains many reaction components, making rapid cooling of the product stream necessary in order to prevent repolymerisation reactions. The pyrolysis oil is nevertheless prone to reactions during storage and heating due to its large content of oxygen (Castello *et al.* 2018). It also contains a lot of water. Further treatment is therefore required to reduce both the oxygen content and reactivity of this oil if it is to be used as fuel (Schutyser *et al.* 2018).

3.3 Oxidation

Taking an oxidative approach to lignin depolymerisation usually results in a product with a high fraction of aldehydes or carboxylic acids, depending on the severity of the reaction (Pandey and Kim 2011). While catalytic approaches with O_2 are used, there are also examples of nitrobenzene, metal oxides and hydrogen peroxide oxidations

(Pandey and Kim 2011). Lignosulphonates are oxidised on a commercial scale by Borregaard in Norway to produce vanillin.

3.4 Hydrothermal methods

Employing hydrothermal methods, which use water as the reaction medium, is another approach to depolymerising lignin. A significant advantage of this technique is that the feedstock does not need to be dried in advance, as is the case in pyrolysis, because the reaction medium is water. Also, the oxygen content of bio-crude produced by hydrothermal methods is lower than that of bio-oil obtained by pyrolysis, since water may act as a hydrogen donor (Castello and Rosendahl 2018). Furthermore, the low cost and non-toxicity of water make it an attractive reaction medium for hydrothermal processing.

A wide range of temperatures has been investigated and, depending on the desired product, the temperature can be regulated. At lower temperatures (200-400 °C), a carbon-like substance is formed in hydrothermal carbonisation whereas at high temperatures (350-700 °C), gasification occurs (Lappalainen *et al.* 2020). A high gasification temperature (>450 °C) favours H_2 production of the lignin, whereas lower temperature favours methane production. A catalyst is normally used at lower temperature gasification. Liquefaction is achieved at temperature levels in between carbonisation and gasification (250-450 °C and 10-35 MPa); depolymerisation is nevertheless complex and care must be taken, or the material will char.

3.4.1 Water as the reaction medium

Water is used not only as a reaction medium in hydrothermal methods but also as a catalyst, or catalyst precursor, as well as a reactant (Kruse and Dahmen 2015). Thermolysis of the lignin linkages occurs in pyrolysis, whereas hydrolysis of the linkages occurs when water is added.

The ionic product of water increases at higher temperatures before it decreases drastically after surpassing the critical point of water at 374.0 °C and 22.06 MPa (Kruse and Dahmen 2015). This means the concentrations of H_3O^+ and OH^- increase in subcritical water near the critical point, thereby favouring ionic reactions such as hydrolysis (Lappalainen *et al.* 2020). At supercritical conditions, on the other hand, radical reactions occur to a greater extent unless the pressure is sufficiently high (Castello *et al.* 2018).

Near-critical water also has a lower dielectric constant than ambient water. It is thus less polar than ambient water and can dissolve less polar substances. Supercritical water has an even lower dielectric constant than near-critical water, in fact, lower than both benzene and pentane. It can therefore dissolve non-polar components simultaneously as salts precipitate. The use of subcritical water in lignin depolymerisation thus makes it possible to use high concentrations of H_3O^+ and OH^-,

as well as a higher solubility of non-polar components, without salts being precipitated, which would be the case with supercritical water (Lappalainen *et al.* 2020).

3.4.2 Capping agents

Lignin depolymerisation under hydrothermal conditions involves many reactions, including hydrolysis and various hydrogenation reactions. However, repolymerisation occurs at the same time, as reactive fragments from the depolymerisation form new bonds. This process can nevertheless be mitigated by additives, known as capping agents, which scavenge the reactive components. Alcohols have usually been employed, but so has boric acid (Roberts *et al.* 2011). Phenol, when used as a capping agent, has been shown to reduce the char yield and scavenge small reaction components to form e.g. alkylated phenol products (Arturi *et al.* 2017; Belkheiri *et al.* 2018a; Saisu *et al.* 2003). In addition, aliphatic alcohols such as MeOH and EtOH also reduce the char yield (Belkheiri *et al.* 2014; Cheng *et al.* 2012, 2016; Lee *et al.* 2016; Sebhat 2016). It is possible that alcohols act as hydrogen donors and also lower the critical temperature and pressure of the reaction mixture (Kang *et al.* 2013; Wu *et al.* 2014). Employing both water and an alcohol, e.g. EtOH or phenol, seems to have a synergistic effect, reducing char levels compared to a pure water or alcohol solution (Lee *et al.* 2016; Okuda *et al.* 2004). The water content ensures a more efficient hydrolysis than a system with pure alcohol. Yoshikawa *et al.* (2013) investigated a BuOH/water system when depolymerising kraft lignin over a silica-alumina catalyst, observing a synergistic effect when BuOH/water were mixed.

While MeOH, EtOH and BuOH have been studied, the use of IPA as a capping agent in HTL has been investigated only scarcely, and even less so in the HTL of kraft lignin. The work of Sebhat (2016), in which kraft lignin was depolymerised in an equal mixture of water and alcohol (MeOH, EtOH or IPA, respectively) is the only example that was found in the literature. In that study, the addition of alcohol shifted the composition of the product from solid to liquid, i.e. less char was produced. Moreover, the use of IPA gave the most identifiable monomers of all the alcohols. An equal mixture of water and isopropanol were used, however, rather than just isopropanol being an additive. Furthermore, the treatment time of 3 h was long, and the temperature was 225 °C which is low for a liquefaction process that is normally run at 250-450 °C (Lappalainen *et al.* 2020). In the context of employing aliphatic alcohols as capping agents, there is thus a gap in knowledge of the effects of using IPA. Conducting investigations into the use of IPA as a capping agent at higher temperature, shorter residence times and lower loadings than those studied by Sebhat (2016) are therefore of interest.

3.4.3 Effect of residence time

The amount of char produced in the hydrothermal depolymerisation of lignin can also be reduced by regulating the residence time in the reactor (Bernhardt *et al.* 2021).

Several studies, employing different types of lignin, are compiled in Table 1, some highlights of which are presented in this section.

An early study was published by Bobleter and Concin who depolymerised Willstätter lignin, an acid hydrolysis lignin, obtained from poplar (Bobleter and Concin 1979). A minimum of solid residue, defined as non-dissolvables in a 10:1 acetone:water mixture, was obtained after 0.4 to 3 min of residence time at 365 and 270 °C, respectively. At longer residence times, the reforming of solids through repolymerisation occurred, although the increase levelled off after 7 min. The authors concluded that the reaction occurred in two stages: rapid initial depolymerisation followed by slower repolymerisation.

Saisu *et al.* depolymerised organosolv lignin with phenol in supercritical water (400 °C) for 10-60 minutes (Saisu *et al.* 2003). The lowest yield of tetrahydrofuran (THF) insolubles, i.e. char, together with the highest yield of oil, i.e. THF solubles, was obtained at 10 min of residence time in the reactor. With increasing residence time, more insolubles were formed and less solubles, but phenol derivates increased with residence time. In another depolymerisation study of organosolv lignin under supercritical conditions (400 °C) with the addition of phenol, Okuda *et al.* noticed a remarkable change in the molecular weight distribution of their THF soluble fractions already after 6 min (0.1 h) of residence time (Okuda *et al.* 2004): these THF soluble fractions composed the entire reaction mixture at 6 min, meaning that no char was formed at this residence time. The profile altered less at longer residence times, indicating that the major change in the structure occurred early in the reaction. As a side note, it can be mentioned that Okuda *et al.* observed an increased capture of carbon by the phenol in the reaction mixture at longer residence times. This concurs with the results obtained for the phenol derivatives by Saisu *et al.* (2003).

Zhang *et al.* (2008) depolymerised five different kinds of lignin, two of which were kraft lignins, in water without any capping agent between 300 and 374 °C. They concluded that the solid fraction remaining after centrifugation of the aqueous reaction product, extracted using acetone, reached a constant value after 12 and 3 min of residence time at 300 and 374 °C, respectively. As the heating-up time was 3 min, the residence time when reaching a constant yield of solid fraction could be assumed to be 15 and 6 min, respectively. A constant value of char yield after these residence times supports the claim later made by Bernhardt *et al.* (2021), i.e. a short reaction is advantageous in reducing the char yield in kraft lignin depolymerisation. The char yield in the study of Zhang *et al.* was around 40 % of the starting lignin.

In two kinetic studies of the depolymerisation of alkaline lignosulfonate in sub and supercritical water, Yong and Matsumura obtained residence times in the order of seconds in their continuous reactor that was 1 mm in diameter (Yong and Matsumura 2013, 2012). They reported complete depolymerisation of the lignin within 5 s in

supercritical cases and 10 s in subcritical cases: the systems used were dilute, containing just 0.1 wt% lignin, to prevent the continuous reactor from plugging. The char yield in the supercritical case increased several times compared to the subcritical case, an effect that was attributed to the radical reactions in the former case.

Cheng *et al.* did not observe any significant influence of the residence time when depolymerising alkaline lignin at 300 °C in the time span of 15-360 min (Cheng *et al.* 2012): the composition of the reaction mixture remained fairly constant. Similarly, Belkheiri did not note any major difference in the yields of oil, water soluble organics (WSO) or char when the approximate residence time was reduced from 11 to 6 min in the continuous reactor set-up (Belkheiri 2018). Nevertheless, the individual compounds shifted considerably, with the guaiacol yield dropping at longer residence times.

Finally, Abad-Fernández *et al.* depolymerised kraft lignin in ultrarapid conditions at both sub and supercritical conditions (Abad-Fernández *et al.* 2020). Like Yong and Matsumura, they used a continuous reactor that was run with a 0.1 wt% lignin solution to avoid plugging (Yong and Matsumura 2013, 2012). At supercritical conditions, 386 and 400 °C, the production of oil, defined as ethyl acetate soluble compounds from the liquid product phase, was noted after 50 ms of reaction; the maximum oil yield was obtained at 386 °C and 170 ms. At subcritical conditions, on the other hand, 2 s of residence time was required to reach the maximum oil yield.

The results of Zhang *et al.* (2008) and Belkheiri (2018) concur for the HTL of kraft lignin: kraft lignin reacts at around 350-374 °C and reaches a rather stable product composition within 6 min (Belkheiri 2018; Zhang *et al.* 2008). The work of Abad-Fernández *et al.* indicates that kraft lignin depolymerises extremely swiftly at both sub and supercritical conditions (Abad-Fernández *et al.* 2020). Abdelaziz *et al.* (2018) show that depolymerisation of kraft lignin occurs within 1 min, with GPC chromatograms at 250 °C without any capping agent, with less change being seen at 170 °C. Although different methods of tracking the reaction were employed in these studies, depolymerisation does appear to happen within minutes in subcritical conditions and seconds for super-critical conditions. Despite this, knowledge of the structural changes that occur in the lignin in at the early part of the reactions remains scarce.

Table 1: Compilation of studies on the influence of residence time on the depolymerisation of lignin.

Study	Lignin	Conc. of lignin [wt%]	Reactor	T [°C]	Residence time [s]	Residence time [min]	Solvent	Pressure [MPa]	Co-solvent/ capping agent	Catalyst	Method used to track depolymerisation
(Bobleter and Concin 1979)	HCl hydrolysis lignin (hardwood)	2	Batch, 8ml	270–372	24–900 (including heating)	0.4–15 (including heating)	Water	Not stated	--	--	Yield of solid residue after 10:1 acetone:water extraction
(Miller et al. 1999)	Organosolv (hardwood) and Indulin AT (Kraft softwood)	Approx. 10	Batch, 14 ml	290	0–3600 (+90 s heating and 30 s additional cooling)	0–60 min (+1.5 min heating and 0.5 min quenching)	EtOH or MeOH	Not stated	--	KOH, NaOH, CsOH, LiOH, $Ca(OH)_2$, and Na_2CO_3	Yield of precipitates at pH 2 washed with water and DEE
(Saisu et al. 2003)	Organosolv lignin	1.5–2	Batch, 10 ml	400	300–3600 (of which 240 s heating + 60 s additional cooling)	5–60 (of which 4 min heating + 1 min additional cooling)	Water	Not stated	Phenol	--	Yield of THF insolubles and THF solubles
(Okuda et al. 2004)	Organosolv lignin	2.2–3.8	Batch, 5 ml	400	360–3600 (+240 s heating)	6–60 (+4min heating)	Water	Estimated at <37	Phenol	--	GPC profile of whole reaction mixture
(Wahyudiono et al. 2008)	Alkaline lignin	3–11	Batch, 5ml	350–400	300–14400 (of which 180 s heating)	5–240 (of which 3 min heating)	Water	25–40	--	--	Yield of MeOH-insolubles (MI)
(Zhang et al. 2008)	2 Kraft lignins (softwood), organosolv lignin from oat hull, 2 acid hydrolysis lignin (hardwood and switchgrass)	10	Batch, 75 ml (induction heating)	300–374	60–1800 (+150-180 s heating + 300 s additional cooling)	1–30 (+2.5-3 min heating + 5 min additional cooling)	Water	10–22	--	--	Yield of solid residue after acetone extraction
(Roberts et al. 2011)	Organosolv lignin	2.5-10	Continuous	240–340	120–900	2–15	Water	25-31.5	--	NaOH	Oil yield (EtAc extract)
(Roberts et al. 2011)	Organosolv lignin	2.5	Batch, 5.6 ml	270–360	1200–3600	20–60	Water	Not stated	Boric acid	NaOH	Oil yield (EtAc extract)
(Cheng et al. 2012)	Alkaline lignin	9–11	Batch, 14 ml and 75 ml	200–450	900–21600 (+60–120 s heating)	15–360 (+1–2 min heating)	Water/EtOH	5 at the beginning, increasing when heated	$H_{2(g)}$	$Ni10/Al_2O_3$, $Ru10/Al_2O_3$, Pt10/AC	Yield of solid residue, degraded lignin, and water-soluble product
(Yong and Matsumura 2012)	Alkaline lignosulfonates (softwood)	0.1	Continuous, 1 mm diameter	390–450	0.5–10	0–0.17	Water	25	--	--	Yield of residual lignin
(Yong and Matsumura 2013)	Alkaline lignosulfonates (softwood)	0.1	Continuous, 1 mm diameter	300–370	0.5–10	0–0.17	Water	25	--	--	Yield of residual lignin
(Rößiger et al. 2017)	Organosolv lignin (hardwood), Kraft lignin (softwood)	Organosolv, 2.5–10, Kraft, 2.5–7.5	Continuous, 2.7 l	240–340	450–900	7.5–15	Water	25	--	NaOH	Oil yield (MIKB extract) and precipitated oligomers
(Abdelaziz et al. 2018)	Kraft lignin (softwood)	5	Continuous, 18 ml heated, 50 ml total	170–250	60–240	1–4	Water	12–13	--	NaOH	GPC profile
(Belkheiri 2018)	Kraft lignin (softwood)	5.5	Continuous, 500 ml	350	360–660	6–11	Water	25	Phenol	$KOH+K_2CO_3$, ZrO_2	Yield of solid residue, bio-oil, and water-soluble organics yield.
(Islam et al. 2018)	Kraft lignin	1.2–9	Batch, 300 ml	200–350	0–3600 (+1200–1800 s heating)	0–60min (+20–30 min heating)	Water	Not stated	--	--	Oil yield (acetone and EtAc extract) and solid residue
(Otromke et al. 2019a)	Kraft lignin (softwood) extracted with MeOH	Approx. 10	Continuous, 50 ml (cf. Otromke *et al.* 2019b)	300	480–1440 s	8–24 min	Water	18	--	NaOH	GPC profile and NMR spectra
(Abad-Fernández et al. 2020)	Kraft lignin	0.1	Continuous, 0.5-12.3 ml	300–400	0.06–4.6	0–0.08	Water	26	--	--	Oil yield (EtAc extract)

4
Materials and Methods

This chapter begins with an account of the HTL treatment of the kraft lignin, followed by a description of the product characterisation. Next, the starting materials are described and finally the test plan of the work is presented.

4.1 HTL treatment

Lignin depolymerisation was carried out in a small, 99 ml, batch reactor (SITEC-Sieber Engineering AG, Zürich, Switzerland) equipped with an injection system comprised of two hand pumps to inject the sample during the run. Wetted parts of the reactor and tubing were all made of Inconel 625, as described by Arturi *et al.* (2017). Figure 7 shows two images of the reactor system: its front is on the left, where the two hand pumps are clearly visible, and its back is on the right, where the reactor vessel can be seen.

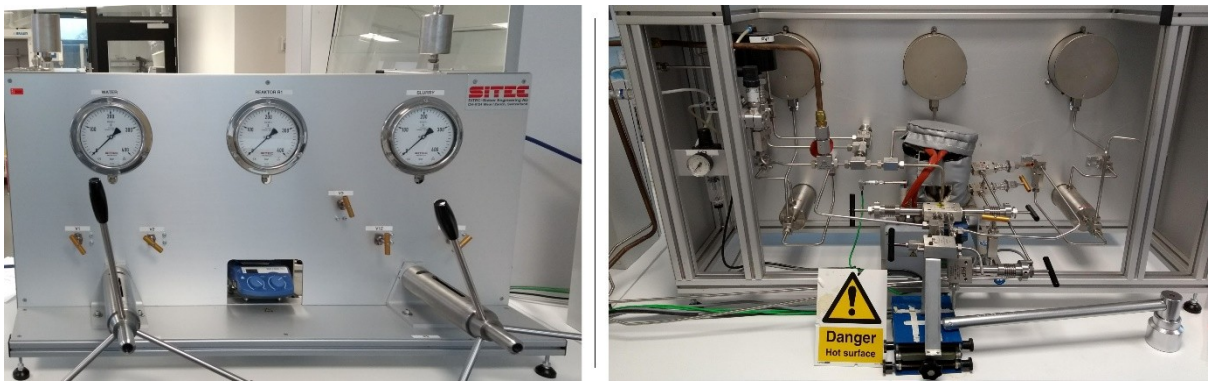

Figure 7: Front (left) and back (right) of the reactor system.

The reaction mixture was prepared in two batches: the pre-charge containing water and Na_2CO_3, and the injection charge containing isopropanol and kraft lignin in addition to the water and Na_2CO_3. The pre-charge, constituting roughly 60 % of the total reaction mixture by weight, was preheated in the sealed reactor to ensure rapid heating of the kraft lignin. Air was displaced using N_2 before the reactor was sealed. When the pre-charge had been heated, the injection charge was injected via a pump (P2 in Figure 8), into the vapour-liquid equilibrium prevailing in the reactor (R1 in Figure 8). Condensing steam thus heated the injection charge and brought the system to the reaction temperature within one minute after injection was complete. The water injection pump (P1) was not used in this work. Once the desired HTL treatment time was reached, the reaction charge was discharged via a valve (V5) into a cold trap of 200 ml water in a flask submerged in ice.

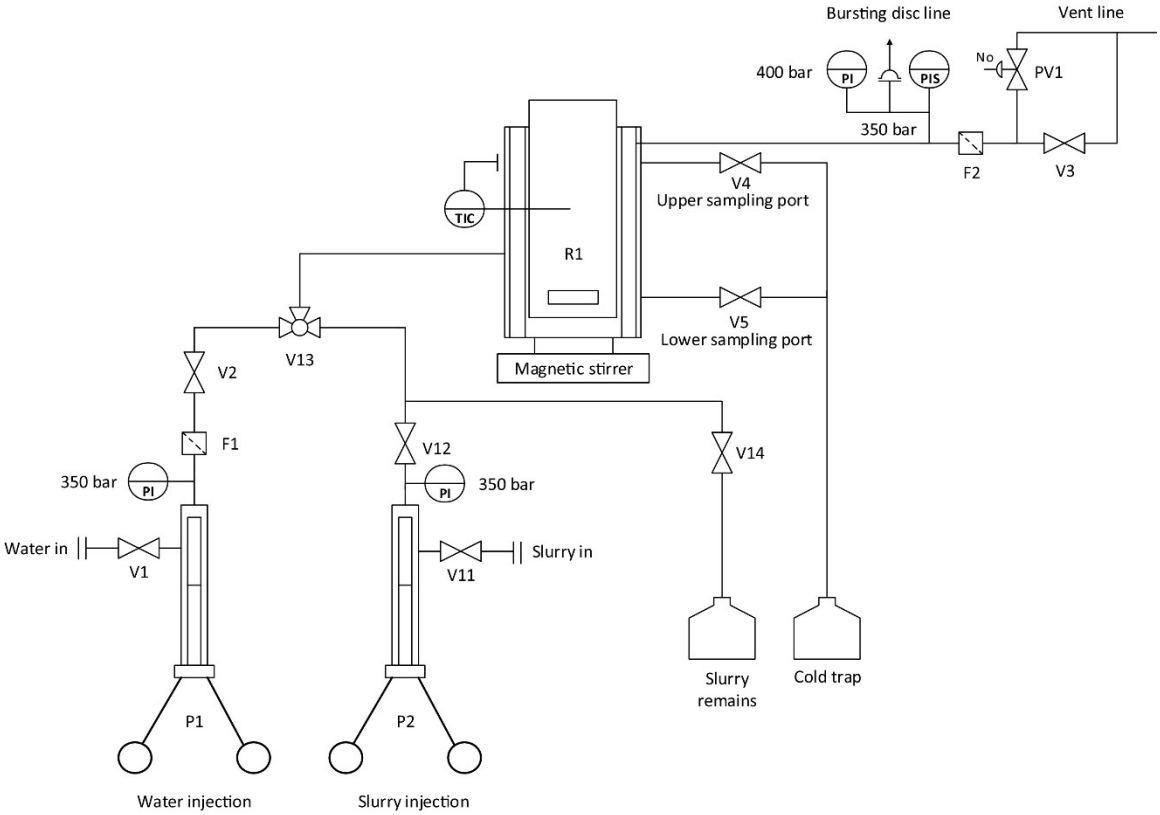

Figure 8: P&I diagram of the reactor system employed in this study.[1]

The reaction product was fractioned into three fractions: char, precipitated solids (PS) and acid soluble organics (ASO). An outline of the fractionation is presented in Figure 9. Firstly, the reaction product was filtered using glass filters with a nominal cut-off of 1.0-1.6 µm. The resulting filter cake was dried for 96 h at 40 °C, after which it was denoted "char". The insolubles in the product phase hence formed the char fraction.

[1] Reprinted from *The Journal of Supercritical Fluids*, 123, K.R. Arturi, M. Strandgaard, R.P. Nielsen, E.G. Søgaard & M. Maschietti. Hydrothermal liquefaction of lignin in near-critical water in a new batch reactor: Influence of phenol and temperature, 28-39, (2017), with permission from Elsevier.

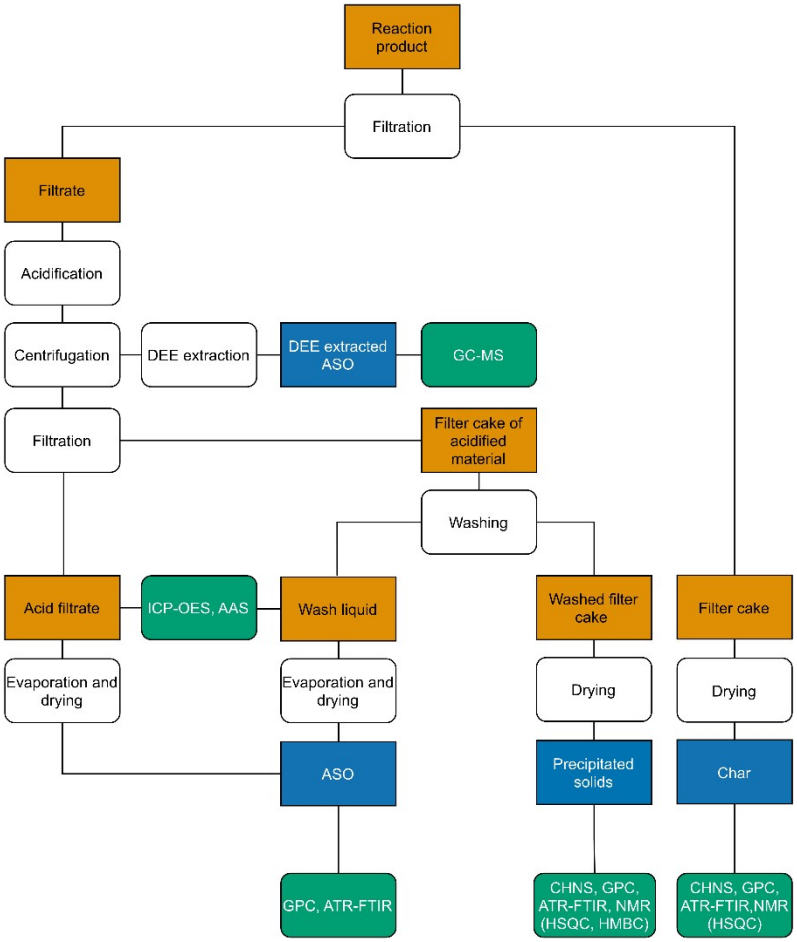

Figure 9: Flowchart of the fractionation of the reaction product and ensuing analyses.

The remaining filtrate was a brown opaque liquid containing soluble organic material. This organic material was precipitated with 1 M HCl under gas evolution, as the remaining carbonates from the added Na_2CO_3 formed CO_2. Lowering the pH precipitated a brown material, leaving a pale-yellow liquid. The mixture comprised of the pale-yellow aqueous phase and precipitated material was filtered with a glass filter at a nominal cut-off of 1.0-1.6 µm and the filtrate stored. The filter cake was thereafter washed with 50 ml of water; subsequent drying of the filter cake, for 120 h at 40 °C, formed the PS fraction. A fraction of the filtrate was extracted with diethyl ether (DEE) at a ratio of 1:1 before being mixed with an internal standard of syringol for subsequent analysis with gas chromatography-mass spectrometry (GC-MS). Evaporating the water in the pale-yellow filtrate, first at ambient conditions for 72 h and then at 40 °C for 24 h, gave the ASO fraction.

4.2 Characterisation of the products

The yields (Y) of the product fractions were investigated gravimetrically and are reported as yields vs. dry lignin added to the reactor thus:

$$Y_i = \frac{m_i}{m_{lig}}$$

where Y_i is the yield of fraction i for the respective reactor run, m_i is the mass of compound i and m_{lig} is the dry weight of the lignin loaded.

4.2.1 Moisture, residual salts and melting points

The moisture content of the lignin ranged from 78.8 to 85.0 % and was determined by a moisture analyser (Sartorius MA30; Sartorius, Göttingen, Germany).

A portion of the dried ASO fraction was salt crystals. Assuming this salt to be NaCl, with Na^+ from the Na_2CO_3 and Cl^- from the added HCl, the content of salt was estimated by measuring the sodium content in the aqueous phase after acidification and filtration using atomic absorption spectroscopy (AAS, Thermo Scientific iCE3000, Thermo Fisher Scientific, Cambridge, UK), and inductively-coupled plasma optical emission spectroscopy (ICP-OES, Thermo Scientific iCAP 6500, Thermo Fischer, Cambridge, UK). The estimated salt content was deducted from the ASO.

The melting points of the solids were investigated with a microscope (Olympus BH-2, Olympus Corporation, Tokyo, Japan) equipped with a heating plate (Mettler FP82HT Hotstage and Mettler FP90, Mettler-Toledo GmBH, Greifensee, Switzerland). The heating rate was 20 °C/min up to a maximum of 375 °C.

4.2.2 Molecular weights

The depolymerisation anticipated during the HTL treatment was tracked by investigating the molecular weights of the fractions using gel permeation chromatography (GPC) in a two-column system (PL-GPC 50 Plus Integrated GPC system, Polymer Laboratories, Varian Inc., Church Stretton, UK) equipped with a guard column. Two detectors were installed in the system, a refractive index (RI) and an ultraviolet light (UV) detector, with the latter operating at 280 nm. Samples were dissolved in the eluent at a concentration of 0.24 mg/ml, filtered using a syringe filter with a cut-off of 0.2 µm and run at 50 °C with the eluent dimethyl sulfoxide (DMSO) with 10 mM LiBr. The system was calibrated with pullulan standards (Varian PL2090-0100, Varian Inc., Church Stretton, UK). Normalisation of the results was made according to:

$$I_{i,n} = \frac{I_i - I_{min}}{I_{max} - I_{\min}}$$

where $I_{i,n}$ is the normalised intensity at point i in the spectrum, I_i is the intensity at point i and I_{min} and I_{max} are the minimum and maximum intensities measured.

4.2.3 Structural changes

Structural changes of the lignin that occurred during the HTL treatment were investigated using nuclear magnetic resonance spectroscopy (NMR, Bruker Avance III HD, Bruker BioSpin GmBH, Rheinstetten, Germany) and attenuated total reflectance Fourier transform infrared spectroscopy (ATR-FTIR, PerkinElmer Frontier FT-IR, PerkinElmer, Inc. Waltham, MA, USA and GladiATR-FTIR, PIKE Technologies, Madison, WI, USA). The ATR-FTIR spectra were recorded as absorbance between 4000 and 400 cm^{-1}, with a 4 cm^{-1} resolution and 10 scans per sample. ASO samples investigated with ATR-FTIR were freeze-dried (FreeZone Triad 7400030 freeze drier; Labconco Corporation, Kansas City, MO, USA) to remove as much water as possible.

Apart from ^{1}H proton spectra, the NMR analyses were comprised of heteronuclear single quantum coherence (HSQC) and heteronuclear multiple bond correlation (HMBC) experiments: the latter as a complement to the former. The HSQC experiments display correlations of a heteroatom (carbon in this case) and protons when connected by a single bond. The HMBC experiments can be used for correlations between heteroatoms and protons over a distance exceeding a single bond. Samples were prepared at a concentration of 140 mg/ml in DMSO-*d6* (35 mg in 0.25 ml solvent). While all the PS dissolved in the solvent, a small fraction of the lignin and char, <5 wt%, did not. The undissolved material was not investigated with NMR, but since it only is a small fraction of the total mass this was deemed not to affect the main conclusions. Two magnets were used, 700 MHz (16.4 T) and 800 MHz (18.8 T), and the pulse sequences employed were *hsqcedetgpsisp2.3* for HSQC, *hmbcetgpl3nd* for HMBC and *zg30* for the ^{1}H spectra. The HSQC spectra were recorded in an edited fashion, i.e. C-H correlations in methine (CH) and methyl (CH_3) units are positive whereas correlations in methylene units (CH_2) are negative.

4.2.4 Elemental analyses

Elemental analyses of the products were made by CHNS combustion analysis in pure oxygen (Elementar vario MICRO cube, Elementar Analysensysteme GmbH, Langenselbold, Germany). Helium was used as the carrier gas in the integrated gas chromatograph (GC). Lignin, char and PS (2 mg pre-dried at 105 °C for a minimum of 12 h) were added to the machine in tin weighing boats. Carbon, nitrogen, hydrogen and sulphur were determined by the analysis, whilst oxygen was calculated from the difference. Sulphanilamide (Elementar Analysensysteme, ≥ 99 %) was used for calibration.

4.2.5 Identification of monomers

Identification and semi-quantification of the components remaining in the aqueous phase after acidification were carried out using gas chromatography mass spectrometry (GC-MS, Agilent 7890A, Agilent Technologies Co. Ltd., Shanghai, China and Agilent 5975C, Agilent Technologies Inc. Wilmington, DE, USA). 1 ml of 10^{-3} g/ml syringol

solution was added to 10 ml of acidified filtrate before the mixture was extracted at a ratio of 1:1 *w/w* with DEE. The DEE phase was filtered with a 0.45 µm syringe filter and then run in the GC-MS. Syringol was chosen as an internal standard since it has a similar structure to the products anticipated, namely phenolic monomers. Syringol should not be formed to any large extent during the HTL treatment because the lignin was sourced from softwood, which is predominantly comprised of coniferyl alcohol, and not sinapyl alcohol, which contains the syringol structure (Gellerstedt 2015). The semi-quantification was made according to Nguyen *et al.* (2014):

$$W_i = W_{IST} \frac{A_i}{A_{IST}}$$

with A being the chromatographic peak area, W the mass fraction in the sample, i the analyte and IST the internal standard (syringol). Identification of the compounds was carried out using the NIST MS Search Programme (Vers. 2.2) employing NIST/EPA/NIH Mass Spectral Library (NIST 11).

4.3 Materials

Softwood kraft lignin sourced from Norway spruce (*Picea abies*) and Scots pine (*Pinus sylvestris*) was used in all the test series. The lignin was isolated using the LignoBoost process at the Bäckhammar Mill in Sweden. The content of sulphur was 2 % in the starting lignin as shown in Table 2. No nitrogen was detected in the starting lignin, which was as expected.

Table 2: Elemental composition of LignoBoost lignin, with standard deviations based on duplicate runs.

	LignoBoost
C [wt%]	68.0±0.0
H [wt%]	5.7±0.0
O[a] [wt%]	24.4±0.1
S [wt%]	1.97±0.2

[a] Oxygen is calculated by difference.

While the preceding kraft pulping break a large fraction of the β-O-4' bonds from the lignin, the HSQC experiments proved that both β-O-4' bonds and other inter-unit ether linkages remained in the lignin because they showed up in the inter-unit aliphatic region of the NMR spectra: δ_C/δ_H 52.5-90/2.8-5.7 ppm. This region is presented in Figure 10, with annotations according to Mattsson *et al.* (2016). Several signals are related to each bond, one for each C-H unit on the alkyl chain: in the case of β-O-4', for example, signals can be seen for C_α-H at δ_C/δ_H 72/4.75 ppm, C_β-H at δ_C/δ_H 85/4.3 ppm and C_γ-H at δ_C/δ_H 60/3.6 ppm. Linkages such as 5-5' and 4-O-5', however, will not show in HSQC due to the lack of a C-H bond to the carbon atoms of these bonds,

cf. Figure 6. Red peaks correspond to C-H correlations in CH or CH_3 moieties, and blue peaks to CH_2.

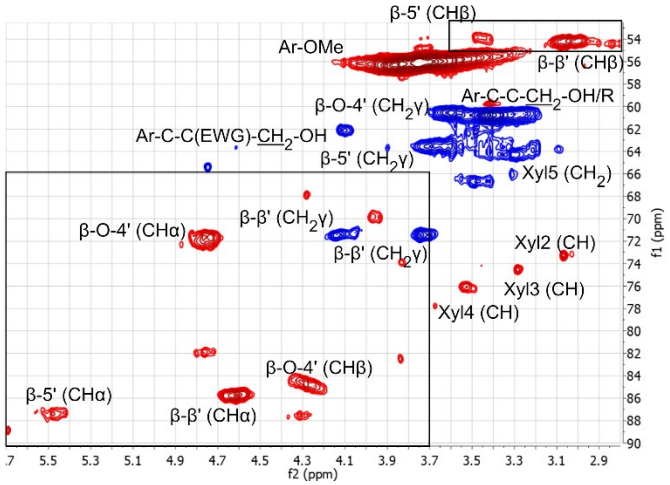

Figure 10: Inter-unit aliphatic region of the HSQC spectrum for unreacted LignoBoost lignin, with annotations according to Mattsson et al. (2016). The specifications within the parentheses denote to which C-H coupling the annotation belongs. EWG: electron-withdrawing group, LCC: lignin carbohydrate complex and Xyl: xylan.

The lignin was depolymerised in deionised water, anhydrous Na_2CO_3 (Merck, ≥99.9% and J.T. Baker, >99.5 %), and IPA (VWR Chemicals, ≥99.8% and VWR Chemicals, >99.9 %). For separation and analysis, syringol (Aldrich, 99%), diethyl ether (Sigma-Aldrich, ≥99.0%, ≥1 ppm BHT as inhibitor, and VWR Chemicals, ≥99.7% stabilised with BHT), NaCl (Merck, ≥99.5%), LiBr (Sigma-Aldrich, ≥99%), DMSO (Sigma-Aldrich, ≥99.7%), DMSO-d6 (Sigma-Aldrich, 99.5 atom% D, 0.03% (v/v) TMS), pullulan standards (Varian, PL2090-0100), HNO_3 (Merck Suprapur, 65 %) and sodium standard (UltraScientific) were used. All chemicals were used as received apart from the 1 M HCl used in acidification, which was diluted in-house (Sharlau, 37%).

4.4 Test plan

Three test series were carried out in this work to investigate the effects of IPA loading measured as the ratio to dry lignin (ranging between 0-4.9 and hereafter called the *IPA series*), temperature (290-335 °C) and residence time in the reactor (1-12 min): these HTL treatment conditions are reported in Table 3. In each of these series, the pressure was 250 bar, the baseline IPA/dry lignin level was 2.7 (*w/w*) and the baseline residence time in the reactor was 12 min. The residence time was defined as the period between the injection being completed and the point at which the reactor discharge began. Thus, the injection time was not included in the residence time. The temperature was 320 °C in the IPA series, whilst a lower temperature of 290 °C was used in the time series. The motivation for this lower temperature was the assumption of slower reactions at a lower temperature which creates better resolution of the process, considering the limitations of the reactor. Although high, the heating rate of the reactor nonetheless limits the lowest possible residence time. With a lower reaction temperature, a better resolution of the reaction course could be anticipated.

The batch reactor set-up entails a transient temperature and pressure behaviour, as opposed to a continuous set-up: this is especially evident when the residence time is low. Estimations of average temperatures and pressures were made according to:

$$\Psi_{avg} = \frac{\int_{t_1}^{t_2} \Psi(t)dt}{(t_2 - t_1)}$$

where t_2 is the time of discharge from the reactor, t_1 is the time when the injection was complete and Ψ is either the temperature or pressure.

In accordance with earlier studies on kraft lignin, a residence time of 12 min was chosen (Belkheiri *et al.,* 2014; Nguyen *et al.,* 2014a, 2014b) and the carbonate content used was 1.6-2.1 % (Belkheiri *et al.,* 2018, 2014).

Table 3: Overview of the HTL treatment conditions. N.B. The 2.7 IPA/dry lignin in the IPA series is the same as the 320 °C in the temperature series. The Ref. *sample was run without lignin.*

IPA/dry lignin [g/g]	Residence time [min]	T [°C]	T_{avg} [°C]	P [bar]	P_{avg} [bar]	pH of reaction product	Na_2CO_3 [wt%]	Water [wt%]	IPA [wt%]	Lignin (dry) [wt%]
IPA Series										
0	12	320	313	250	250	8.7	1.6	92.9	0.0	5.5
0.6	12	320	314	250	248	8.7	1.6	88.9	3.6	5.9
2.7	12	320	321	250	248	9.2	1.6	80.7	12.9	4.8
4.9	12	320	314	250	243	9.0	1.6	69.3	24.2	4.9
Ref.	12	320	319	250	242	9.2	1.6	85.0	13.4	0.0
Temperature Series										
2.7	12	290	293	250	256	8.9	1.6	78.0	14.9	5.5
2.7	12	320	321	250	248	9.2	1.6	80.7	12.9	4.8
2.7	12	335	334	250	248	9.2	1.6	80.6	13.0	4.8
Residence Time Series										
2.7	1	290	276	250	227	9.61	2.1	79.4	13.5	5.0
2.7	2	290	284	250	247	9.26	2.1	81.4	12.0	4.5
2.7	4	290	289	250	247	9.29	1.6	80.6	13.0	4.8
2.7	12	290	292	250	246	9.70	2.1	80.5	12.7	4.7

5
Results and Discussion

This chapter begins with an overview of the general results obtained from the HTL treatment of kraft lignin in terms of depolymerisation and the results from the characterisations: examples are taken from all the test series. The trends seen in the results regarding the IPA charging, temperature and residence times follow and, finally, a tentative model of the reaction progression is presented.

5.1 Product appearance and elemental composition

The HTL treatment of softwood kraft lignin in alkaline solution, with isopropanol added as a capping agent, resulted in an opaque brown-black liquor with some solid material and a strong smoky smell; it is presented in Figure 11A. There was only one single liquid phase present in this brown-black suspension. The precipitation brought by acidification is shown in Figure 11B and the filtrated acidified solution in Figure 11C.

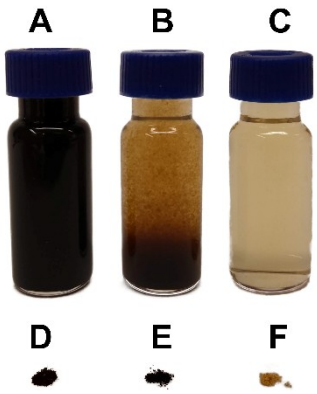

Figure 11: Product fractions: reaction product (A), acidified reaction product (B), filtrated acidified product (C), char (D), PS (E) and ASO (F).

The fractionation of the product outlined in Figure 9 yielded the char and PS as two dark brown to black powders, shown as D and E, respectively, in Figure 11. Evaporation and drying of the liquid phase obtained after acidification yielded an orange-brown coloured solid material, the ASO, and is shown as F in the same figure.

No organic liquid phase was produced in this work as opposed to similar studies in which phenol was used as the capping agent instead of isopropanol (Arturi *et al.,* 2017; Belkheiri *et al.,* 2014; Nguyen *et al.,* 2014b). This might be due to isopropanol being water-soluble to a larger degree than phenol, and therefore not forming a separate phase with a higher affinity for the organic products formed during the reaction.

The elemental analyses of the IPA series are reported in Table 4. The carbon content of the char and PS fractions increases somewhat during the HTL treatment, whereas the hydrogen and oxygen levels decrease to some extent when compared to the starting lignin. After the treatment, the sulphur concentration drops below the level of accurate quantification in both the char and PS fraction, which concurs with the findings of Nguyen *et al.* (2014b).

Table 4: Elemental composition, with standard deviations, of the lignin (LignoBoost), char and PS fraction in the IPA series.

IPA/dry lignin [g/g]	C [wt%]	H [wt%]	O[a] [wt%]	S [wt%]
Char				
LignoBoost	68.0±0.0	5.7±0.0	24.4±0.1	1.97±0.2
0	72.3±0.1	4.8±0.0	22.9±0.1	<0.8[b]
0.6	73.5±0.5	4.9±0.0	21.6±0.5	<0.8[b]
2.7	73.8±2.0	5.1±0.1	21.1±2.1	<0.8[b]
4.9	70.6±0.0	5.0±0.0	24.4±0.1	<0.8[b]
PS				
LignoBoost	68.0±0.0	5.7±0.0	24.4±0.1	1.97±0.2
0	71.3±0.0	4.8±0.0	23.9±0.0	<0.8[b]
0.6	70.0±0.1	4.8±0.0	25.3±0.1	<0.8[b]
2.7	72.5±0.1	5.0±0.0	22.5±0.1	<0.8[b]
4.9	72.9±0.1	5.2±0.0	21.9±0.1	<0.8[b]

[a] Oxygen is calculated by difference. [b] Trace amounts below the limit for accurate quantification.

5.1.1 Changes in molecular structure

Neither the PS nor the char melted when heated up to 375 °C in contrast to the lignin, which melted at around 190 °C. This is a strong indication that structural changes occurred during the HTL treatments: the product fractions were investigated using NMR to elucidate these structural changes further. The inter-unit aliphatic region of the HSQC spectra of the untreated kraft lignin is presented in Figure 12A, with peak annotations according to Mattson *et al.* (2016). Figure 12B and C show the same region for the char and PS, respectively, after 1 min of residence time in the reactor. The ASO fraction was not investigated with NMR. These figures show that the inter-unit ether bonds present in the lignin, Figure 12A, are not found in either the char or the PS. Consequently, these inter-unit ether bonds are broken during the HTL treatment. Furthermore, the β-5' and β-β' bonds both contain a carbon-oxygen (C-O) bond in addition to their respective carbon-carbon (C-C) bond (see Figure 6). Although these C-O bonds break in the char and only traces of the signal remain in the PS (Figure 12C), it is not conclusive that the C-C bond of the β-5' and β-β' linkages also breaks (Mattsson *et al.,* 2016). Nonetheless, these results show that even at 290 °C the depolymerisation reactions are rapid since the inter-unit ether bonds are broken already within 1 min; at higher temperatures, the depolymerisation is likely to be even faster.

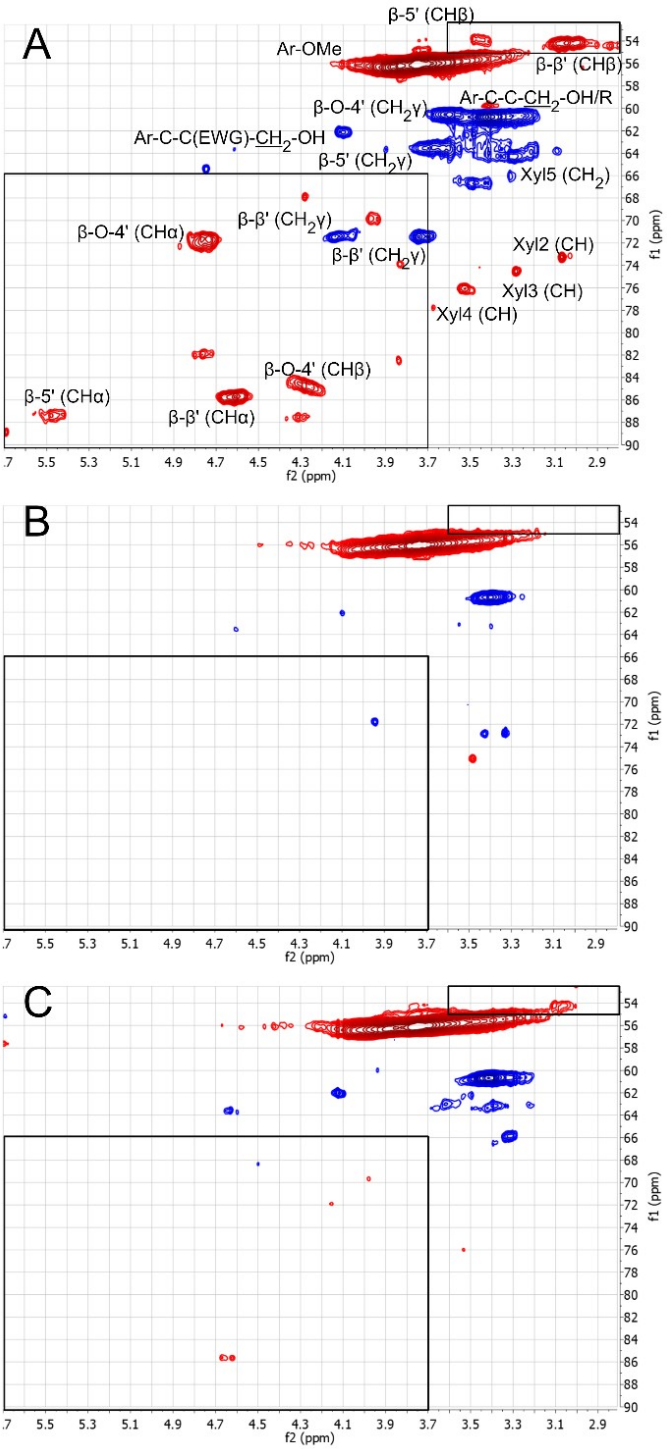

Figure 12: Inter-unit aliphatic region of the HSQC spectra for unreacted LignoBoost lignin (A), char (B) and PS (C) after 1 min of HTL treatment (290 °C, IPA/dry lignin = 2.7). Annotations in the LignoBoost lignin spectrum (A) are made according to Mattsson et al. (2016) and Crestini et al. (2017). *The specifications within the parentheses in (A) denote to which C-H coupling the annotation belongs. EWG: electron-withdrawing group. Xyl: xylan.*

The aliphatic region of the HSQC spectra, namely δ_C/δ_H 10-55/0-2.9, ppm shows the aliphatic C-H bonds that are not connected to oxygen, typically in the propyl side chain of the lignin structure. Also, the solvent peak, DMSO-*d6*, appears at 40/2.5ppm. Residual extractives and fatty acids from the wood in the kraft lignin would appear in

this aliphatic region, but their concentrations are expected to be low (Mattsson *et al.,* 2016). In Figure 13, this region is seen for the same samples, with a 1 min residence time at 290 °C, as those shown in Figure 12. It may be noted that the char fraction, Figure 13B, has fewer peaks in this region compared to both the lignin and the PS. The PS retains most of the peaks from the lignin, suggesting the side chains of the original lignin remain relatively intact in this fraction during HTL treatment.

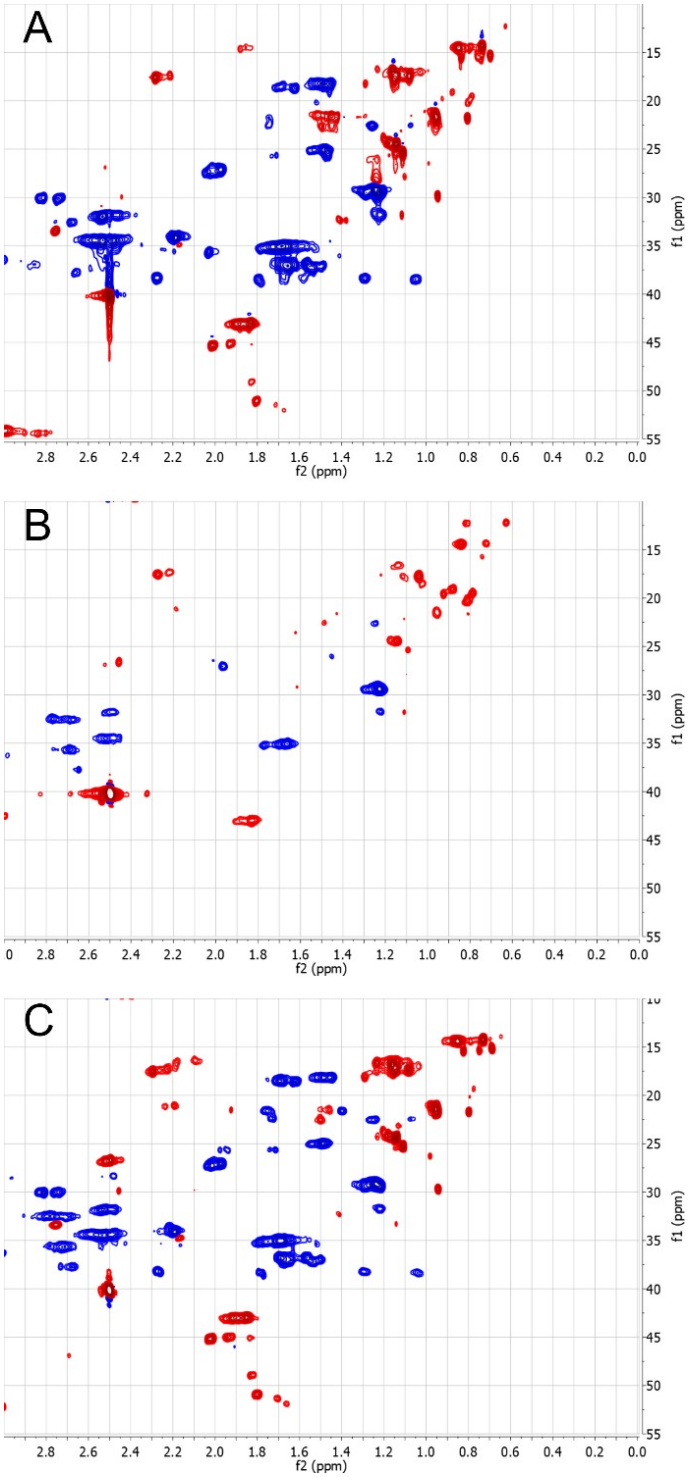

Figure 13: Aliphatic region of the HSQC spectra for LignoBoost lignin (A), char (B) and PS (C) after 1 min of HTL treatment (290 °C, IPA/dry lignin = 2.7).

5.1.2 Changes in molecular weight

The structural changes that occur in lignin during HTL treatment suggest that the molecular weight may also change. Figure 14 presents the molecular weight distributions of the char (A), PS (B) and ASO (C) for the various ratios of IPA to dry lignin. All the fractions have a substantially lower molecular weight than the original lignin. Furthermore, the high molecular weight fractions in the lignin, i.e. exceeding 40 kDa, have virtually disappeared for the PS and ASO. In the char fraction, however, higher molecular weight fractions appear until the amount of IPA is increased to 2.7. The removal of such high molecular weight fractions in the lignin is recurrent through all the experimental series. Altogether, this demonstrates that lignin is depolymerised to various extents during HTL treatment. The effect had by the addition of an IPA on the molecular weight of the lignin is elaborated further in the section "Effect of IPA loading".

The ASO fraction, i.e. organics soluble in the acidified product phase, is mainly comprised of components with a molecular weight lower than that of the char and PS. This is evident from its markedly different molecular weight distribution, which is much richer in lower molecular weight compounds. It is nevertheless surprising that the ASO also has a fraction of higher M_w component: up to about 10 kDa (Figure 14C). The ASO fraction thus contains not only monomers but also larger molecules.

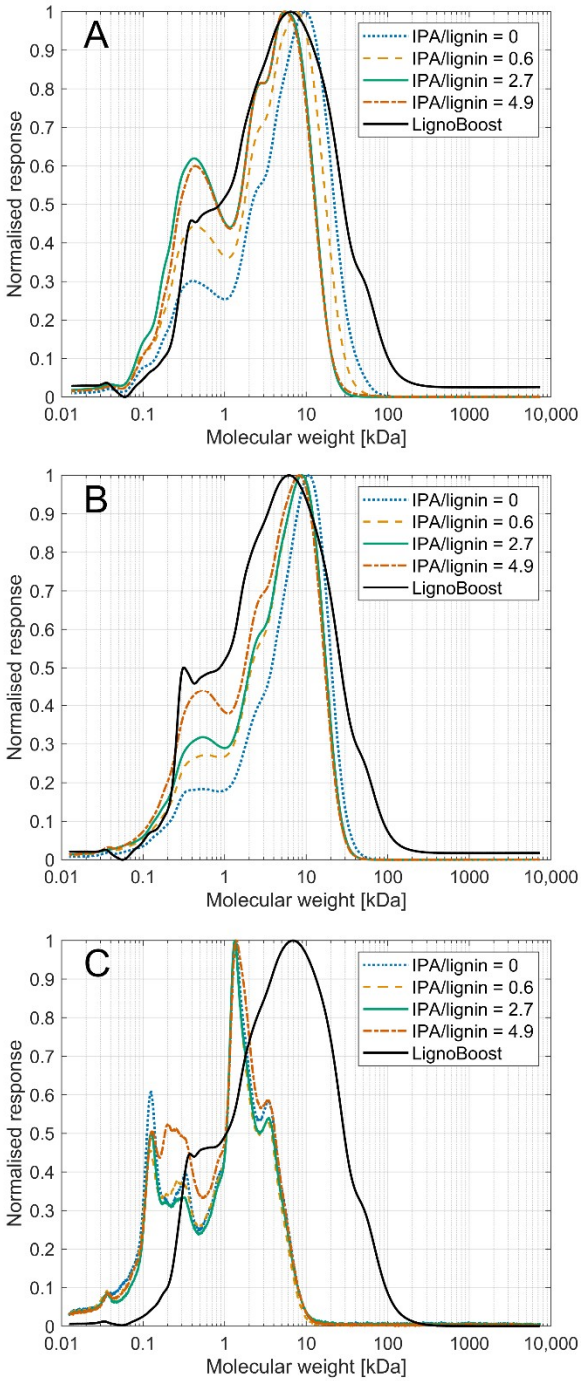

Figure 14: GPC chromatograms in the IPA series for the char (A), PS (B) and ASO (C) fraction after 12 min of HTL treatment at 320 °C.

5.1.3 Char and PS precipitation

The weight average molecular weight (M_w) of the product fractions is also presented in Table 5 in the section "Effect of IPA loading". Despite being dissolved, the PS fraction has an M_w equal to, or higher than, the char fraction (which precipitates). The functional groups of the fractions were investigated with ATR-FTIR, as well as with follow-up measurements with NMR, to examine why the char precipitates while PS and ASO remain dissolved. These NMR measurements employed both HMBC and ^{1}H

NMR pulse sequences. Figure 15 provides the ATR-FTIR spectra of the different fractions after 12 min of HTL treatment at 290 °C. The PS and ASO fractions show a clear carbonyl peak around 1700 cm^{-1}. The ASO also show pronounced peaks for OH groups, which resonate at 3042 to 3695 cm^{-1} (Faix 1992).

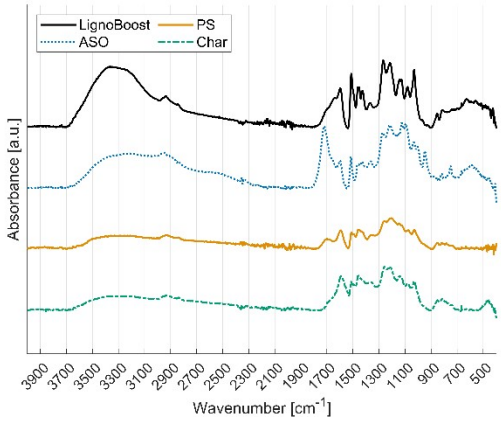

Figure 15: ATR-FTIR spectra of the lignin and product fractions for 12 min of HTL treatment at 290 °C, with an IPA/dry lignin of 2.7.

Figure 16 shows the results obtained from the HMBC experiment on the LignoBoost lignin (A) and PS (B) after 4 min of residence time. The carbonyl presence of the PS fraction seen in Figure 15 is confirmed by the HMBC results, where there are clear cross peaks between carbonyl carbon peaks and aliphatic protons. These cross peaks, which indicate that the side chains have carbonylic carbons, are marked with black rectangles in the figure. McClelland *et al.* (2017) denoted peaks in this region as carboxylic acids and esters. While the HMBC experiment thus confirmed the presence of carbonyl moieties in the PS fraction, it did not provide any usable signals for the char fractions, which could be due to char agglomerates quenching the signal.

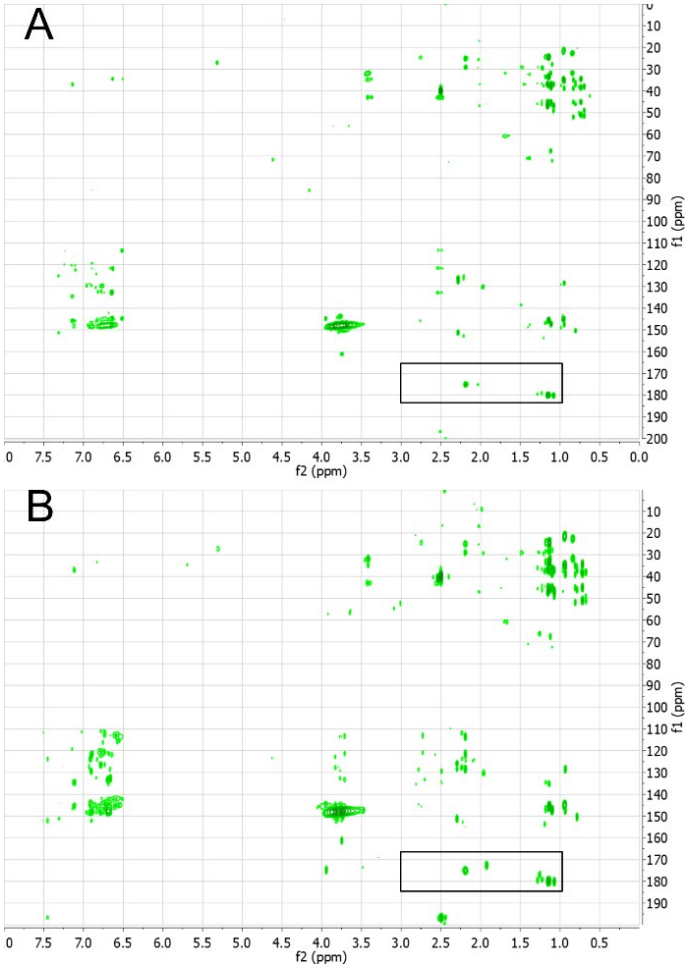

Figure 16: HMBC spectra of LignoBoost lignin (A) and PS (B) after 4 min of HTL treatment at 290 °C and an IPA/dry lignin ratio of 2.7. Carbonyl groups are located within the black rectangles (McClelland *et al.*, 2017).

The ^{1}H spectra of the PS fractions in the temperature series are shown in Figure 17. There are broad peaks in the carboxyl region, i.e. 12-13 ppm, which supports the notion of carboxylic acids units being present in the PS fraction. The protons of the carboxyl group typically exchange with deuterium from the deuterated solvent, making such broad peaks common for carboxylic acids.

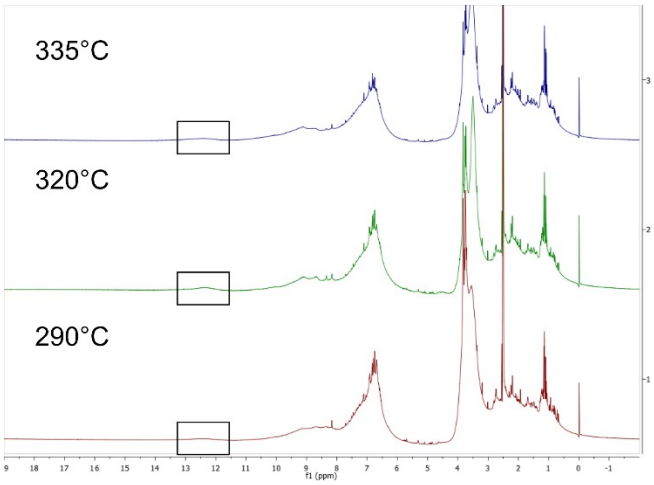

Figure 17: ^{1}H spectra of the PS in the temperature series with a HTL treatment of 12 min and an IPA/dry lignin of 2.7. The weak broad peaks (black boxes) represent carboxylic acids.

The results of the ATR-FTIR, HMBC and ^{1}H measurements suggest a content of polar groups in the PS and the ASO fraction. Such groups, e.g. carbonyl and, to some extent, the OH groups, would retain the PS fraction dissolved prior to acidification. Protonation of the carboxylic acids in the PS when acidifying the sample would thus cause precipitation to occur. The ASO, on the other hand, remain dissolved despite protonation due to the content of other polar groups.

The HMBC results further indicate that the carbonyl units of the PS fraction are located on the aliphatic side chain: there are cross-peaks between the carbonyl carbons and aliphatic protons in the black boxes in Figure 16 but not between the carbonyl carbons and aromatic protons at 170-180/6-8 ppm. Moreover, studies carried out by González *et al.* (2004) on model compounds have shown that carboxylic acids on aromatic rings decarboxylate rapidly under hydrothermal conditions. It thus appears that the carbonyl units are placed on the aliphatic side chain rather than on the aromatic rings. The aliphatic region of the NMR spectra, Figure 13, reveals that the PS peaks are not only more numerous than those of the char fraction, but also that they are of higher intensity. This indicates that the aliphatic side chains are retained to a larger extent in the PS fraction. The presence of carbonyl and other functional groups on the aliphatic side chain could allow the PS fraction to be kept solubilised, due its greater amount of aliphatic units bearing functional groups, as opposed to the precipitated char fraction. Given that the carbonyl units keeping the PS fraction solubilised are situated on the aliphatic side chains, cleavage of these side chains from the aromatic units would cause precipitation and the yield of char, with fewer aliphatic groups, would thereby increase.

5.1.4 Monomeric products

A subset of the ASO is comprised of small molecules that were identified by GC-MS; these are displayed in Figure 18. They are typically phenolic components with the major product being guaiacol (2-methoxy phenol), which is Molecule **2** in Figure 18. This result was expected since the starting material was softwood lignin: such lignin is comprised mainly of coniferyl alcohol, which contains guaiacol moieties.

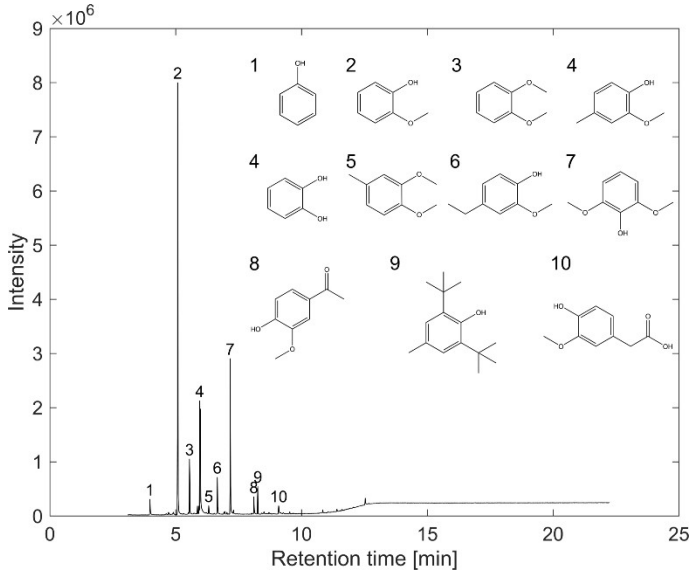

Figure 18: Typical gas chromatography (GC) chromatogram of the ASO extracted by DEE. Peak 4 is a mixture of creosol and catechol and therefore not properly resolved, Peak 7 is the internal standard (syringol) and Peak 9 is the solvent preservative BHT (butylated hydroxytoluene).

Comparing the yield of monomers obtained in the test series carried out here with similar experiments using phenol instead of isopropanol as the capping agent in the same reactor, the amount of quantified components are the same: up to 4 wt% (Arturi *et al.,* 2017). However, the work of Arturi *et al.*, as well as another investigation into the HTL of kraft lignin using phenol as a capping agent, showed significantly more phenol derivates than in the present study (Arturi *et al.* 2017; Nguyen *et al.* 2014a). This is probably due to the fact that many of the monomers identified by GC-MS in the works of Arturi *et al.* and Nguyen *et al.* did not originate primarily from the lignin structure, but were instead added phenol alkylated with reactive components emanated from the lignin degradation process (Saisu *et al.,* 2003). No apparent alkylation with the added isopropanol was observed among the monomers in this work, i.e. no isopropyl chains were noted on the monomers. The alkyl phenols detected, labelled **4** and **6** in Figure 18**,** had shorter alkyl groups instead, namely methyl and ethyl groups. These groups are substituted *para* to the hydroxyl group, suggesting that these are shortened propyl chains from the lignin monomers cf. Figure 1. It thus seems as though some breaking of C-C bonds occurs in the side chain during HTL treatment.

5.1.5 Summary

General observations made of HTL treatment may be summarised as follows: the product fractions showed clear structural changes compared to the original lignin; the inter-unit ether linkages were cleaved; and the molecular weights were reduced as the fractions with the highest molecular weight disappeared. Furthermore, no melting of the char or the PS fractions occurred at temperatures up to 375 °C (unlike the original lignin material) and no apparent oil phase was produced in this set-up.

The aliphatic region in the NMR spectra of the char fraction was much less pronounced than in the PS fraction, indicating a lower amount of aliphatic components in the char. In addition, the PS and ASO contained both polar carbonyl and OH groups, which kept them solubilised in the aqueous product suspension.

Monomers are formed during HTL treatment, with guaiacol being the most common. Moreover, ASO contains not only the small monomeric molecules but also a fraction of high molecular weight components.

5.2 Effect of IPA loading

The yields of the product fractions obtained in the IPA series are shown in Figure 19. The char yield reduces as the level of IPA increases, whilst those of the soluble components, PS and ASO, increase.

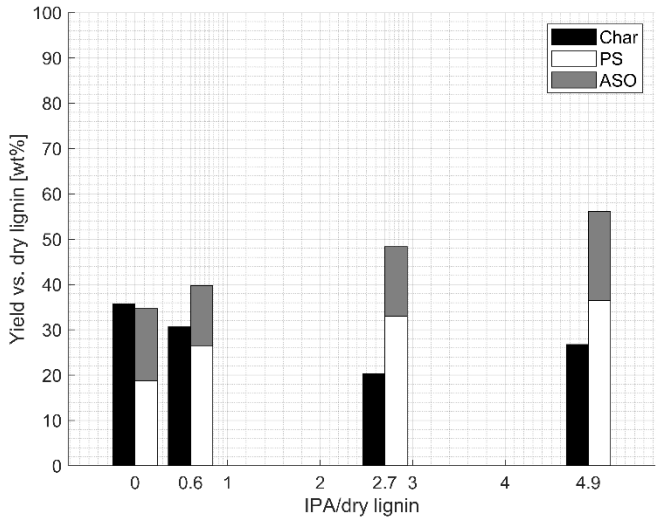

Figure 19: Yields of product fractions vs. IPA/dry lignin ratio after 12 min of HTL treatment at 320 °C.

The molecular weight distributions of the product fractions in the IPA series displayed in Figure 14 show that the peak position shifts towards lower molecular weight fractions with increasing IPA loading. Lower molecular weight compounds also increase with IPA loading, as seen by the increase in the left peak in Figure 14A and B. The weight average molecular weights (M_w) of the product fractions, reported in Table 5, are consequently reduced compared to the starting lignin, and increasingly so as the IPA loading increases.

Table 5: Weight average molecular weights (M_w), with standard deviations, of the product fractions in the IPA series.

IPA/dry lignin [g/g]	Char [kDa]	PS [kDa]	ASO [kDa]	LignoBoost [kDa]
0	8.21±0.04	8.34±0.03	1.66±0.01	11.38±0.08
0.6	5.83±0.01	6.44±0.01	1.56±0.00	
2.7	4.03±0.01	6.37±0.03	1.69±0.02	
4.9	4.14±0.00	5.65±0.01	1.58±0.00	

The reduced char yield and reduced molecular weights with increasing IPA concentration suggest the IPA to have a capping effect. Although the exact mechanisms behind this capping effect of IPA remain unknown, it is likely that the reactive fragments in the product mixture are stabilised by hydrogen donations made by the IPA, similarly to when other alcohols are employed (Wu *et al.,* 2014). However, as was shown in the elemental composition in Table 4, there is no clear effect on the elemental composition when the IPA level is increased within the range investigated, even though the HTL treatment itself causes the carbon contents of both the char and PS to increase compared to the original lignin. Neither is there any trend evident in the yield of ASO components identified by GC-MS with increasing IPA level.

5.3 Effect of reaction temperature

The yields of the product fractions in the temperature series are presented in Figure 20. The yield of char increases with temperature while that of the PS fraction decreases: the yield is thus shifted from PS to char.

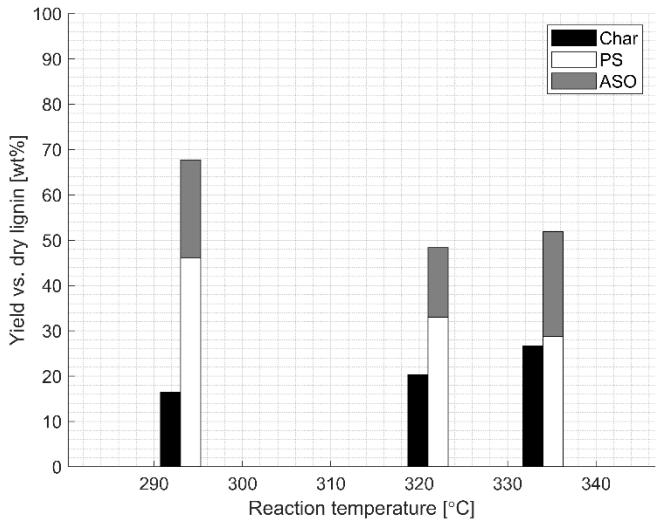

Figure 20: Yields of reaction products vs. average reaction temperature after 12 min of HTL treatment with IPA/dry lignin 2.7 (w/w).

The GPC chromatograms in the temperature series are shown in Figure 21: char (A), PS (B) and ASO (C). It is clear that the high molecular weight fractions in the lignin, i.e. exceeding 40 kDa, decrease in all product fractions. However, while the char gains

a larger fraction of the lower molecular weight compounds, as seen by the left peak in Figure 21A, the ASO lose such components when the temperature increases, Figure 21C. The PS also lose lower molecular weight components but to a much lesser extent than the ASO.

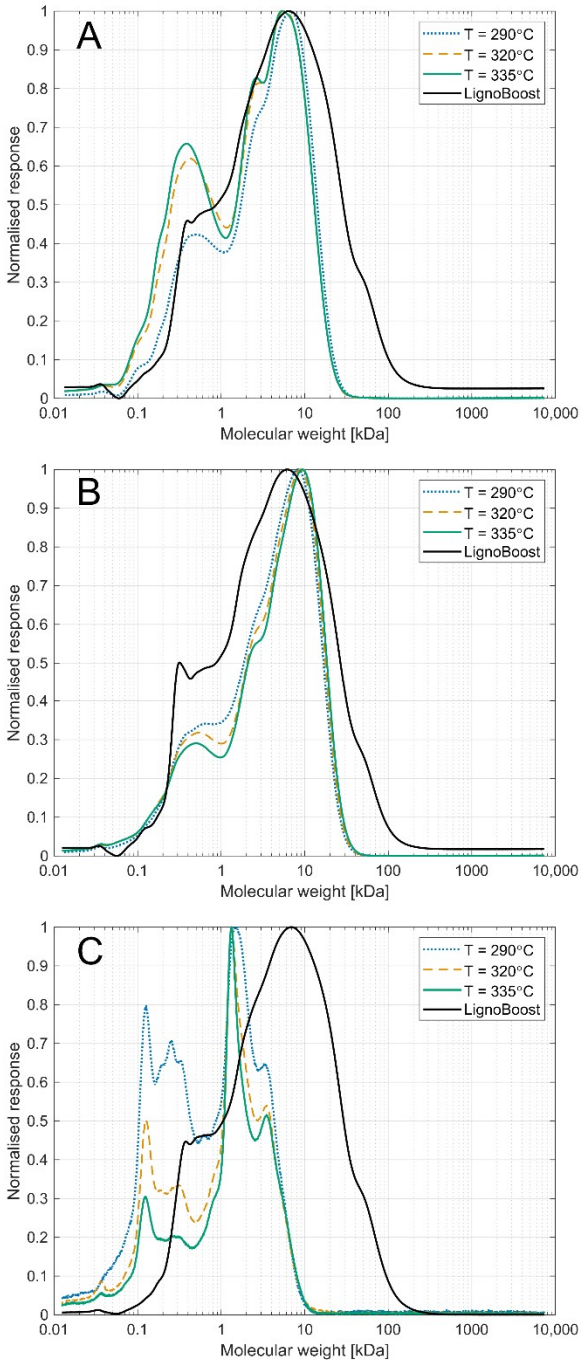

Figure 21: GPC chromatograms in the temperature series for the char (A), PS (B) and ASO (C) fractions after 12 min of HTL treatment with IPA/dry lignin 2.7 (w/w).

These changes are also seen in the weight average molecular weights (M_w) presented in Table 6. As in the IPA series, the M_w of the PS is higher than the char and, while the M_w of char decreases with increasing temperature, it increases for both PS and

ASO. The char yield thus increases, and M_w of char decreases with increasing temperature. One possible explanation is that with increasing reaction temperature the reaction kinetics shifts towards promoting cleavage of polar groups from the PS fraction which causes more char to form while the yield of PS decreases. Larger char fragments degrade to a higher extent at higher temperature which is seen by the reduction of the M_w for the char. Simultaneously, the higher temperature causes the remaining PS fraction to repolymerise. Another possibility is that the cleavage of polar groups from the PS fractions could by hypothesised to occur on the smaller PS molecules, meaning the PS fraction is enriched in large fragments, while the char fraction obtains a higher degree of small molecules, lowering the M_w. Consequently, the difference in molecular weight between the char and PS increases with reaction temperature.

Table 6: Weight average molecular weights (M_w), with standard deviations, of the product fractions in the temperature series.

Reaction temperature [°C]	Char [kDa]	PS [kDa]	ASO [kDa]	LignoBoost [kDa]
290	4.86±0.00	5.96±0.00	1.38±0.00	
320	4.03±0.01	6.37±0.03	1.69±0.02	11.38±0.08
335	3.94±0.01	6.77±0.01	1.89±0.00	

The elemental compositions of the products in the temperature series are given in Table 7. The carbon content of the char fraction shows the largest change in the temperature series: with increasing temperature it increases from 68.0 wt% of the original lignin to 76.1, while the oxygen level drops from 24.4 to 18.7 wt%. Although more char, with a higher carbon content, is thus produced as the temperature increases, it has a lower molecular weight. The elemental composition of the PS fraction, on the other hand, does not show any clear trend with increased temperature. In addition, no evident trend connected to increasing temperature is noticeable with respect to the yield of the ASO monomers identified by GC-MS.

Table 7: Elemental composition, with standard deviations, of the lignin (LignoBoost), char and PS fraction in temperature series.

Sample	C [wt%]	H [wt%]	O[a] [wt%]	S [wt%]
		Char		
LignoBoost	68.0±0.0	5.7±0.0	24.4±0.1	1.97±0.2
290 °C	70.1±0.6	5.1±0.1	24.9±0.7	<0.8[b]
320 °C	73.8±2.0	5.1±0.1	21.1±2.1	<0.8[b]
335 °C	76.1±0.1	5.2±0.0	18.7±0.0	<0.8[b]
		Precipitated Solids		
LignoBoost	68.0±0.0	5.7±0.0	24.4±0.1	1.97±0.2
290 °C	72.3±0.2	5.2±0.0	22.6±0.2	<0.8[b]
320 °C	72.5±0.1	5.0±0.0	22.5±0.1	<0.8[b]
335 °C	70.9±0.4	4.8±0.0	24.3±0.3	<0.8[b]

[a] Oxygen is calculated by difference. [b] Trace amounts below the limit for accurate quantification.

5.4 Effect of residence time

The repolymerisation that occurs in the reaction mixture makes it of interest to limit the residence time in the reactor and investigate the behaviour of the reaction system in the early phases of the HTL treatment. As shown in Figure 22, the yield of char increases with increasing residence time in the reactor at 290 °C. The amounts of dissolved components, PS and ASO, decrease with increasing residence time, suggesting that they contribute to the formation of char instead.

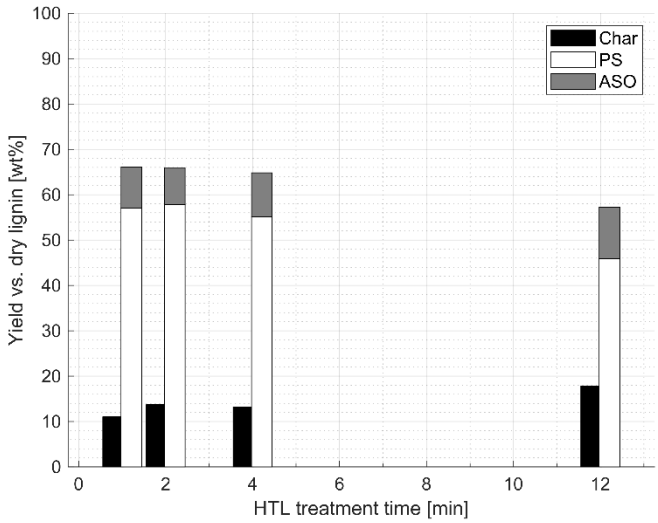

Figure 22: Yields of reaction products vs. HTL treatment time. Run at 290 °C with IPA/dry lignin 2.7 (w/w).

The HSQC spectra in Figure 12 shows that inter-unit bonds were broken within 1 min of residence time. Whilst some weak signals, and particularly those of the β-β' bond, remain at δ_C/δ_H 86/4.65 ppm in the PS spectrum (Figure 12C), these residual signals vanish at longer residence times. The inter-unit ether linkages are therefore broken. This structural change occurs rapidly: within 1 min of HTL treatment.

The weight average molecular weight (M_w) of the product fractions in the time series is presented in Table 8. After only 1 min of HTL treatment, the M_w is at least halved for all fractions compared to the starting lignin.

Table 8: Weight average molecular weights (M_w) of the product fractions in the residence time series, with their respective standard deviation.

Residence time [min]	Char [kDa]	PS [kDa]	ASO [kDa]	LignoBoost [kDa]
1	5.88±0.01	5.85±0.01	1.68±0.02	12.2±0.4
2	5.42±0.01	4.58±0.00	1.30±0.02	
4	4.69±0.00	4.47±0.01	1.18±0.01	
12	6.05±0.00	4.71±0.00	1.32±0.01	

As found in the IPA (Figure 14) and temperature (Figure 21) series, the larger lignin fractions, with a molecular weight exceeding 40 kDa, vanished almost completely after just 1 min of residence time, see Figure 23.

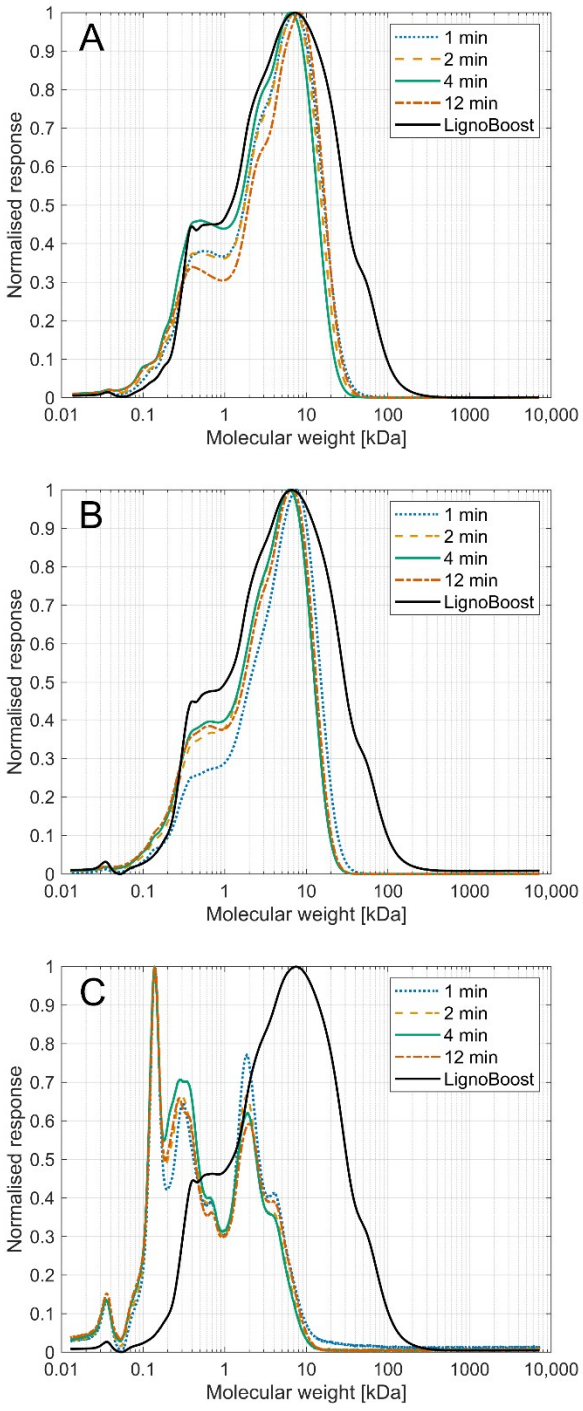

Figure 23: GPC chromatograms of the HTL treatment time series: char (A), PS (B) and ASO (C). Run at 290 °C with IPA/dry lignin 2.7 (w/w).

Consequently, the conclusion is that depolymerisation occurs rapidly at the beginning of the HTL treatment, as evidenced by the changes in structure and molecular weight. Nevertheless, Table 8 shows that the weight average molecular weight increases

between 4 and 12 min of HTL treatment for all the fractions, especially char. The depolymerisation rate is thus exceeded by repolymerisation at longer residence times.

While the ether-based bonds are broken under the conditions used in this study, the char and PS fractions retain a high molecular weight. C-C bonds are generally stronger than C-O bonds (Parthasarathi *et al.,* 2011; Shuai *et al.,* 2016), and it is possible that many of these C-C bonds withstand depolymerisation at this temperature. However, the evident reduction in M_w at residence times between 1 and 4 min (Table 8) means that at least some of these C-C bonds must be cleaved at longer residence times, since hardly any C-O inter-unit linkages remain to be broken after 1 min. The breaking of C-C bonds is supported further by the notion that the char has fewer aliphatic units, as seen in Figure 13. Since the yield of char increases with residence time, this indicates that more side aliphatic chains are cleaved from the lignin structure via C-C scission.

ATR-FTIR spectra of the product fractions in the time series were recorded in order to investigate changes in the functional groups during the reactions. The results are presented in Figure 24: char (A), PS (B) and ASO (C). After 1 min of HTL treatment, there is a definite change in the spectra compared to the starting lignin, but longer residence times do not make as pronounced changes for any of the product fractions as the initial 1 min of residence time. It seems that only minor changes occur after the initial reactions, providing further evidence to support the notion of rapid depolymerisation of kraft lignin. The small changes that occur after the initial reactions concur with the small changes in the M_w at longer residence times, see Table 8. Although these changes in M_w are clear, they are rather modest in comparison with the initial reaction, like the changes in the ATR-FTIR spectra in Figure 24.

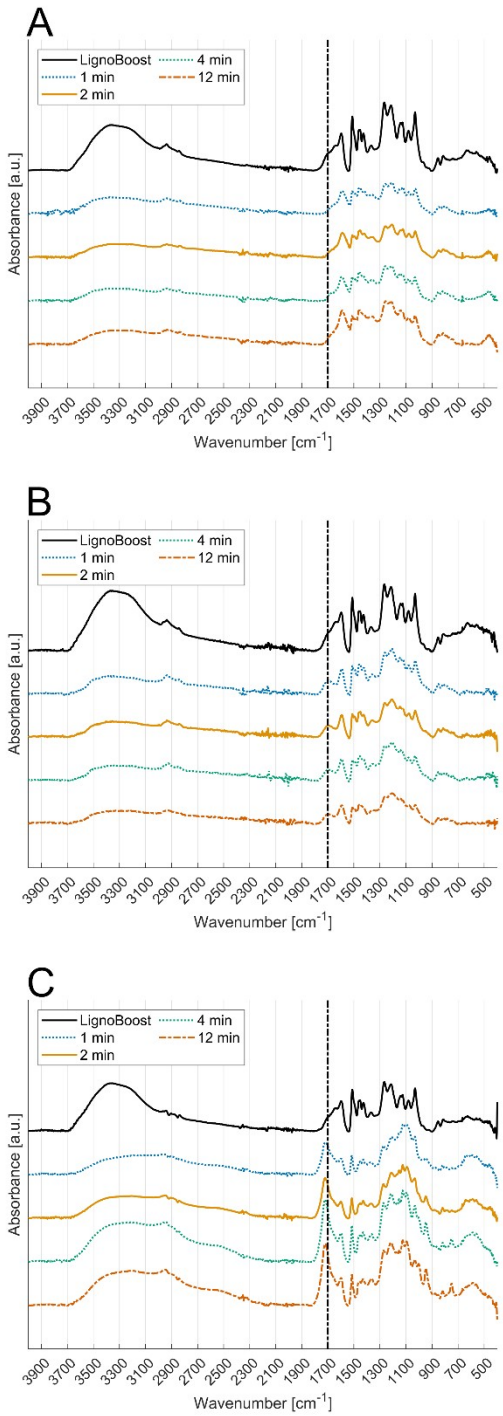

Figure 24: ATR-FTIR spectra in the HTL treatment time series: char (A), PS (B) and ASO (C), with the 1700 cm^{-1} carbonylic wave number marked by the dashed vertical line. Run at 290 °C with IPA/dry lignin 2.7 (w/w).

The results obtained from the investigation of low-molecular weight compounds identified by GC-MS in the time series are presented in Figure 25. Although only a semi-quantitative method was used, it is clear that all identified monomeric products

increased with residence time. It is possible that this may be due to the cleavage of C-C bonds liberating monomeric units at longer residence times.

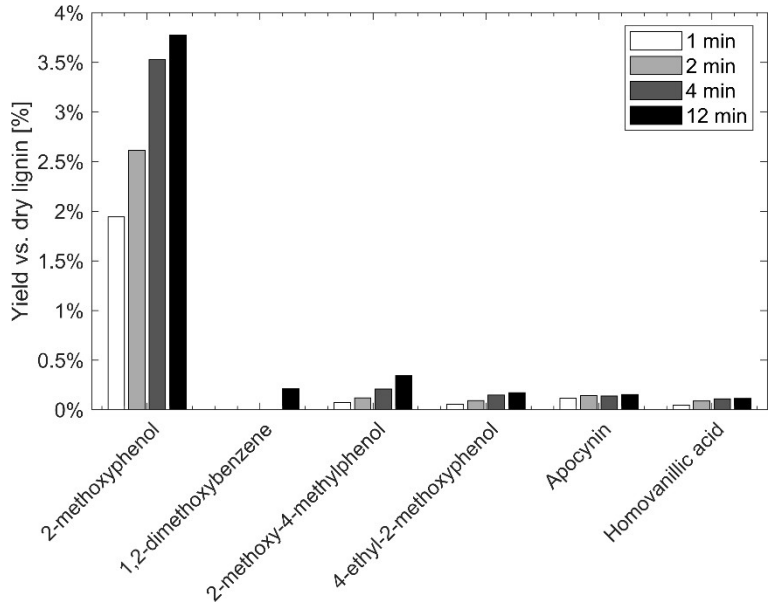

Figure 25: The most prevalent compounds identified by GC-MS in the time series run at 290 °C with IPA/dry lignin 2.7 (w/w), and their respective yield vs. lignin added (determined semi-quantically).

5.5 Tentative reaction progression

Several reactions occur during the HTL treatment of kraft lignin, running on different time scales. The NMR analyses showed that the inter-unit C-O linkages broke within 1 min and thereby caused a dramatic change in the M_w. Longer residence times also affected the M_w, probably by the cleavage of more recalcitrant C-C bonds and, subsequently, by repolymerisation. The change in M_w at longer residence times in the reactor, however, was not as significant as in the initial reactions.

Product molecules of different sizes are formed, evidenced by the wide molecular weight distributions given in Figure 14, Figure 21 and Figure 23. In addition, small one-ring aromatics are formed, as identified by GC-MS. Some parts of the products react further, albeit at a slower rate than the initial breaking of C-O linkages, whilst other parts are stable. Whilst the reacting products lead to higher M_w at long residence times, more monomers are also formed at these longer times. As the reactions proceed at longer residence times, more char is produced. It is possible that the char forms through the precipitation of material when side chains having polar groups that solubilise molecules are cleaved off from molecules in the PS fraction and large molecules in the ASO fraction. The resulting molecules agglomerate and precipitate as char.

A tentative overview of the reaction progressions, based on the fractionation and analyses of the reaction product, is shown in Figure 26. The swift reaction from lignin to form a product which may be fractioned into char, PS and ASO, is followed by reactions that shift the yield from PS and ASO to char, as seen in Figure 22. At

intermediate residence times, net cleavage of bonds in the structure reduces the molecular weights of the product fractions, whereas at longer residence times, repolymerisation reactions become more prominent and the M_w increases.

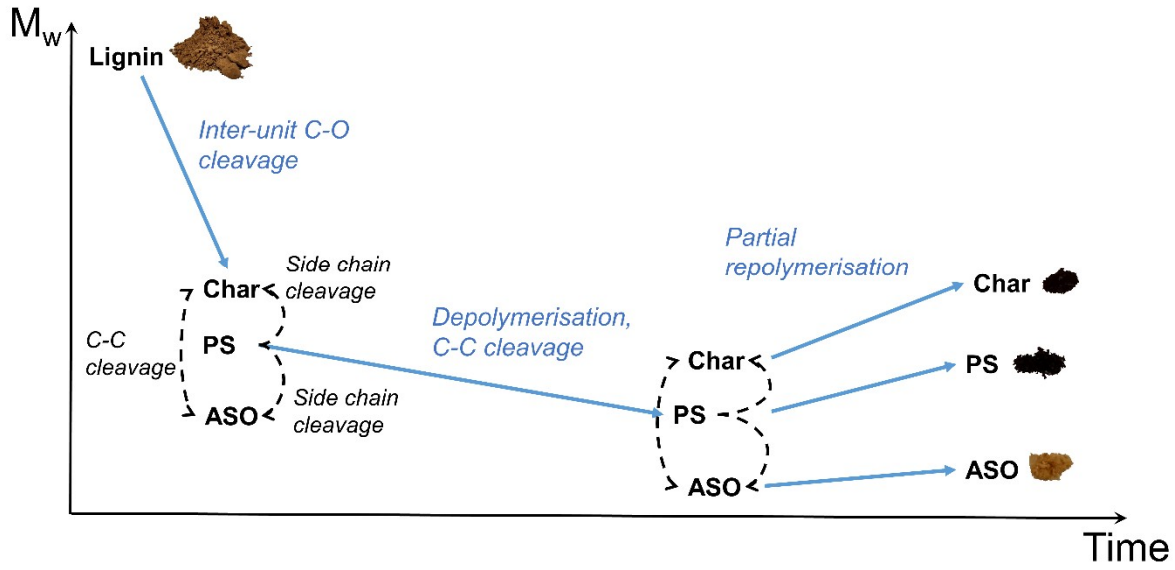

Figure 26: Tentative reaction overview of the HTL treatment employed.

6
Conclusions

The HTL depolymerisation of kraft lignin in a mixture of water, isopropanol and Na_2CO_3, yields a liquid product with a suspended material, char, without any second organic liquid phase. The major product of the process is a water-soluble fraction, PS, which precipitates upon the addition of an acid that protonates its carboxylic acid functionalities. A second fraction, ASO, remains soluble; it contains monomeric units, the most prevalent of which is guaiacol.

Increasing the loading of IPA decreases the molecular weight of the char and shifts the yield from char to PS, thus confirming that isopropanol functions as a capping agent in the process. It reduces both the char yield and the molecular weight of the product fractions, probably by reacting with reactive components that would otherwise have repolymerised during the HTL process. Increasing the reaction temperature increases the amount of char produced. Also, carbon content of the char increases with temperature while its molecular weight decreases.

Kraft lignin is depolymerised swiftly, as the inter-unit ether linkages are broken within 1 min of HTL treatment. Moreover, the molecular weight of all product fractions is at least halved. Increasing the residence time further decreases the molecular weights of the products. At longer residence times of between 4 and 12 min, however, the rate of repolymerisation is faster than that of depolymerisation: this means there is a net repolymerisation, as shown by the increase in molecular weight. It also increases the

char yield and, at the same time, the content of the monomeric molecules identified by GC-MS increases, too. At this temperature of 290 °C, the residence time can thus be fine-tuned to reduce the char content, although care needs to be taken so that the content of monomers is not reduced excessively.

7
Future Work

Although the addition of isopropanol in this work was shown to reduce char yields and molecular weights, it failed at producing an organic liquid phase that similar studies, employing phenol as the capping agent, rendered. Such a separation of phases is beneficial from a separation perspective in a tentative large scale HTL process. However, since the miscibility of water and IPA make the formation of such an organic phase unlikely, another type of capping agent, one that is less soluble in water, could be employed instead. Extraction of organic components could thus occur, like when Yoshikawa *et al.* (2013) used butanol as a capping agent.

Another avenue that could be of interest to explore is the use of glycerol. This has not, to the author's knowledge, been employed as a capping agent in kraft lignin depolymerisation, although examples using aspen wood, algae and rice straw exist (Cao *et al.,* 2016; Han *et al.,* 2019; Pedersen *et al.,* 2016, 2015). Crude glycerol is produced as a side stream in the production of bio-diesel making investigation into the feasibility of its use as a capping agent in the HTL of kraft lignin interesting. However, the good solubility of glycerol in water may impede phase separation after the HTL process, as was the case with the IPA utilised in this work. This could be overcome using by a ternary system of water (for the hydrolysis), alcohol (for the capping effect) and an organic solvent (for the formation of an organic phase after the reaction). The organic solvent would thus be added along with water and alcohol.

Another approach could be to investigate extraction of the HTL product with ethyl acetate (EtAc). The yield of bio-oil is commonly-defined as the components extractable by EtAc (Orebom *et al.,* 2018). Employing this method could be a way of producing and evaluating the production of bio-oil from the process. The use of an extra organic solvent in the reaction could thereby be omitted.

8
Acknowledgements

The financial support received from The Swedish Energy Agency for this work is gratefully acknowledged. I wish to thank the following people sincerely, without whom this thesis would not have been possible:

- Professor Hans Theliander, my main supervisor, for taking me on as a Ph.D. student and guiding me through this process, with scientific discussions and support.
- Associate Professor Merima Hasani, my co-supervisor, for her scientific input and continuous support.
- Associate Professor Marco Maschietti, for giving me the opportunity to use the reactor at Aalborg University in Denmark, and all fruitful discussions we had.
- Dr. Huyen Lyckeskog, for introducing me to the hydrothermal liquefaction of kraft lignin and teaching me how to operate the GC-MS.
- Associate Professor Rudi Nielsen, for all his help with operating the reactor at Aalborg University.
- Dr. Ulrika Brath, for her skilful help with the NMR measurements, and Associate Professor Diana Bernin for the ensuing NMR discussions.
- Ms. Dorte Spangsmark, for her help in the laboratory at Aalborg University.
- Associate Professor Sven-Ingvar Andersson, for teaching me how to operate the AAS and for his continuous input to this project.

- ❖ Dr. Stefan Gustafsson, for teaching me how to operate the CHNS equipment, and Dr. Stellan Holgersson for conducting the ICP-OES measurements.
- ❖ Ms. Maureen Sondell, for her linguistic review of this thesis and its appended papers.
- ❖ Dr. Tor Sewring, for his guidance during the start of my Ph.D. studies and, together with Mr. Kenneth Arandia, for making our shared office such a pleasant place to work in.
- ❖ All my colleagues at SIKT: present and former Ph.D. students, research engineers, administrative staff and post-docs, for making the 3rd floor such a nice workplace.
- ❖ Ms. Anna Lidén and Mr. You Wayne Cheah, for making teaching "Transport Phenomena" such a delight.

Last, but not least come my dear family and friends, for their continuous and unconditional support during this process. Thank you so much!

9 References

Abad-Fernández, N., Pérez, E., Martín, Á. and Cocero, M.J. (2020). Pre-proof Kraft lignin depolymerisation in sub- and supercritical water using ultrafast continuous reactors. Optimization and Reaction Kinetics. J. Supercrit. Fluids 165: 104940. https://doi.org/10.1016/j.jmst.2019.11.010

Abdelaziz, O.Y., Li, K., Tunå, P. and Hulteberg, C.P. (2018). Continuous catalytic depolymerisation and conversion of industrial kraft lignin into low-molecular-weight aromatics. Biomass Convers. Biorefinery 8: 455–470. https://doi.org/https://doi.org/10.1007/s13399-017-0294-2

Arturi, K.R., Strandgaard, M., Nielsen, R.P., Søgaard, E.G. and Maschietti, M. (2017). Hydrothermal liquefaction of lignin in near-critical water in a new batch reactor: Influence of phenol and temperature. J. Supercrit. Fluids 123: 28–39. https://doi.org/10.1016/j.supflu.2016.12.015

Balakshin, M.Y., Capanema, E.A., Sulaeva, I., Schlee, P., Huang, Z., Feng, M., Borghei, M., Rojas, O.J., Potthast, A. and Rosenau, T. (2021). New Opportunities in the Valorization of Technical Lignins. ChemSusChem 14: 1016–1036. https://doi.org/10.1002/cssc.202002553

Belkheiri, T. (2018). Hydrothermal liquefaction of lignin in sub-critical water to produce biofuel and chemicals. Doktorsavhandlingar vid Chalmers tekniska högskola. Ny serie: 4384. Chalmers University of Technology.

Belkheiri, T., Andersson, S.-I., Mattsson, C., Olausson, L., Theliander, H. and Vamling, L. (2018a). Hydrothermal liquefaction of kraft lignin in sub-critical water: the influence of

the sodium and potassium fraction. Biomass Convers. Biorefinery 8: 585–595. https://doi.org/10.1007/s13399-018-0307-9

Belkheiri, T., Andersson, S.-I., Mattsson, C., Olausson, L., Theliander, H. and Vamling, L. (2018b). Hydrothermal Liquefaction of Kraft Lignin in Subcritical Water: Influence of Phenol as Capping Agent. Energy & Fuels 32: 5923–5932. https://doi.org/10.1021/acs.energyfuels.8b00068

Belkheiri, T., Mattsson, C., Andersson, S.I., Olausson, L., Amand, L.E., Theliander, H. and Vamling, L. (2016). Effect of pH on Kraft Lignin Depolymerisation in Subcritical Water. Energy & Fuels 30: 4916–4924. https://doi.org/10.1021/acs.energyfuels.6b00462

Belkheiri, T., Vamling, L., Nguyen, T.D.H., Maschietti, M., Olausson, L., Andersson, S.-I., Åmand, L.-E. and Theliander, H. (2014). Kraft lignin depolymerization in near-critical water: effect of changing co-solvent. Cellul. Chem. Technol. 48: 813–818.

Berlin, A. and Balakshin, M. (2014). Industrial Lignins: Analysis, Properties, and Applications. In: Gupta, V.K., Tuohy, M.G., Kubicek, C.P., Saddler, J., and Xu, F. (Eds.). *Bioenergy Research: Advances and Applications*. Elsevier, Amsterdam, pp. 315–336. https://doi.org/10.1016/B978-0-444-59561-4.00018-8

Bernhardt, J.J., Rößiger, B., Hahn, T. and Pufky-Heinrich, D. (2021). Kinetic modeling of the continuous hydrothermal base catalyzed depolymerization of pine wood based kraft lignin in pilot scale. Ind. Crops Prod. 159: 113119. https://doi.org/10.1016/j.indcrop.2020.113119

Björk, M., Rinne, J., Nikunen, K., Kotilainen, A., Korhonen, V., Wallmo, H. and Karlsson, H. (2015). Successful Start-up of Lignin Extraction at Stora Enso Sunila Mill. In: Hytönen, E. (Ed.). *NWBC 2015 The 6th Nordic Wood Biorefinery Conference*. VTT Technical Research Centre of Finland Ltd, Espoo, pp. 185–192.

Bobleter, O. and Concin, R. (1979). Degradation of poplar lignin by hydrothermal treatment. Cellul. Chem. Technol. 13: 583–593.

Cao, L., Zhang, C., Hao, S., Luo, G., Zhang, S. and Chen, J. (2016). Effect of glycerol as co-solvent on yields of bio-oil from rice straw through hydrothermal liquefaction. Bioresour. Technol. 220: 471–478. https://doi.org/10.1016/j.biortech.2016.08.110

Castello, D., Pedersen, T.H. and Rosendahl, L.A. (2018). Continuous hydrothermal liquefaction of biomass: A critical review. Energies 11:. https://doi.org/10.3390/en11113165

Castello, D. and Rosendahl, L. (2018). Coprocessing of pyrolysis oil in refineries. In: Rosendahl, L.B.T.-D.T.L. for E.A. (Ed.). *Direct Thermochemical Liquefaction for Energy Applications*. Woodhead Publishing, pp. 293–317. https://doi.org/https://doi.org/10.1016/B978-0-08-101029-7.00008-4

Cheng, S., Wilks, C., Yuan, Z., Leitch, M. and Xu, C. (2012). Hydrothermal degradation of alkali lignin to bio-phenolic compounds in sub/supercritical ethanol and water-ethanol co-solvent. Polym. Degrad. Stab. 97: 839–848. https://doi.org/10.1016/j.polymdegradstab.2012.03.044

Cheng, Y., Zhou, Z., Alma, M.H., Sun, D., Zhang, W. and Jiang, J. (2016). Direct liquefaction

of alkali lignin in methanol and water mixture for the production of oligomeric phenols and aromatic ethers. J. Biobased Mater. Bioenergy 10: 76–80. https://doi.org/10.1166/jbmb.2016.1572

Crestini, C., Lange, H., Sette, M. and Argyropoulos, D.S. (2017). On the structure of softwood kraft lignin. Green Chem. 19: 4104–4121. https://doi.org/10.1039/c7gc01812f

Daniel, G. (2009). Wood and Fibre Morphology. In: Ek, M., Gellerstedt, G., and Henriksson, G. (Eds.). *Wood Chemistry and Wood Biotechnology Volume 1 Wood Chemistry and Wood Biotechnology*. Walter de Gruyter GmbH & Co. KG, Berlin, pp. 45–70.

Dessbesell, L., Paleologou, M., Leitch, M., Pulkki, R. and Xu, C. (Charles) (2020). Global lignin supply overview and kraft lignin potential as an alternative for petroleum-based polymers. Renew. Sustain. Energy Rev. 123: 109768. https://doi.org/10.1016/j.rser.2020.109768

Gellerstedt, G. (2015). Softwood kraft lignin: Raw material for the future. Ind. Crops Prod. 77: 845–854. https://doi.org/10.1016/j.indcrop.2015.09.040

Gellerstedt, G. (2009). Chemistry of Chemical Pulping. In: *Pulping Chemistry and Technology*. De Gruyter, Berlin, Boston, pp. 91–120.

Gellerstedt, G. and Henriksson, G. (2008). Lignins: Major Sources, Structure and Properties. In: Belgacem, M.N., and Gandini, A. (Eds.). *Monomers, Polymers and Composites from Renewable Resources*. Elsevier, Amsterdam, pp. 201–224. https://doi.org/https://doi.org/10.1016/B978-0-08-045316-3.00009-0

Gellerstedt, G., Tomani, P., Axegård, P. and Backlund, B. (2013). Lignin recovery and lignin-based products. In: Christopher, L. (Ed.). *Integrated Forest Biorefineries–Challenges and Opportunities*. Royal Society of Chemistry, Cambridge, pp. 180–210.

González, G., Salvadó, J. and Montané, D. (2004). Reactions of vanillic acid in sub- and supercritical water. J. Supercrit. Fluids 31: 57–66. https://doi.org/10.1016/j.supflu.2003.09.015

Han, Y., Hoekman, K., Jena, U. and Das, P. (2019). Use of co-solvents in hydrothermal liquefaction (HTL) of microalgae. Energies 13:. https://doi.org/10.3390/en13010124

Henriksson, G. (2009). Lignin. In: Ek, M., Gellerstedt, G., and Henriksson, G. (Eds.). *Pulp and Paper Chemistry and Technology Volume 1 Wood Chemistry and Wood Biotechnology*. Walter de Gruyter GmbH & Co. KG, Berlin, pp. 121–146.

Huang, X., Korányi, T.I., Boot, M.D. and Hensen, E.J.M. (2015). Ethanol as capping agent and formaldehyde scavenger for efficient depolymerization of lignin to aromatics. Green Chem. 17: 4941–4950. https://doi.org/10.1039/c5gc01120e

Islam, M.N., Taki, G., Rana, M. and Park, J.H. (2018). Yield of Phenolic Monomers from Lignin Hydrothermolysis in Subcritical Water System. Ind. Eng. Chem. Res. 57: 4779–4784. https://doi.org/10.1021/acs.iecr.7b05062

Kang, S., Li, X., Fan, J. and Chang, J. (2013). Hydrothermal conversion of lignin: A review. Renew. Sustain. Energy Rev. 27: 546–558. https://doi.org/https://doi.org/10.1016/j.rser.2013.07.013

Kim, K.H., Brown, R.C., Kieffer, M. and Bai, X. (2014). Hydrogen-donor-assisted solvent liquefaction of lignin to short-chain alkylphenols using a micro reactor/gas chromatography system. Energy and Fuels 28: 6429–6437. https://doi.org/10.1021/ef501678w

Kleinert, M., Gasson, J.R. and Barth, T. (2009). Optimizing solvolysis conditions for integrated depolymerisation and hydrodeoxygenation of lignin to produce liquid biofuel. J. Anal. Appl. Pyrolysis 85: 108–117. https://doi.org/10.1016/j.jaap.2008.09.019

Kruse, A. and Dahmen, N. (2015). Water - A magic solvent for biomass conversion. J. Supercrit. Fluids 96: 36–45. https://doi.org/10.1016/j.supflu.2014.09.038

Lange, J.P. (2018). Lignocellulose Liquefaction to Biocrude: A Tutorial Review. ChemSusChem 11: 997–1014. https://doi.org/10.1002/cssc.201702362

Lappalainen, J., Baudouin, D., Hornung, U., Schuler, J., Melin, K., Bjelić, S., Vogel, F., Konttinen, J. and Joronen, T. (2020). Sub- and Supercritical Water Liquefaction of Kraft Lignin and Black Liquor Derived Lignin. Energies 13: 3309. https://doi.org/10.3390/en13133309

Lee, H.-S., Jae, J., Ha, J.-M. and Suh, D.J. (2016). Hydro- and solvothermolysis of kraft lignin for maximizing production of monomeric aromatic chemicals. Bioresour. Technol. 203: 142–149. https://doi.org/10.1016/j.biortech.2015.12.022

Li, J., Henriksson, G. and Gellerstedt, G. (2007). Lignin depolymerization/repolymerization and its critical role for delignification of aspen wood by steam explosion. Bioresour. Technol. 98: 3061–3068. https://doi.org/10.1016/j.biortech.2006.10.018

Lora, J. (2008). Industrial Commercial Lignins: Sources, Properties and Applications. In: Belgacem, M.N., and Gandini, A. (Eds.). *Monomers, Polymers and Composites from Renewable Resources*. Elsevier, Amsterdam, pp. 225–241. https://doi.org/https://doi.org/10.1016/B978-0-08-045316-3.00010-7

Macfarlane, A.L., Mai, M. and Kadla, J.F. (2014). Bio-based chemicals from biorefining: Lignin conversion and utilisation, Advances in Biorefineries: Biomass and Waste Supply Chain Exploitation. https://doi.org/10.1533/9780857097385.2.659

Mattsson, C., Andersson, S.I., Belkheiri, T., Åmand, L.E., Olausson, L., Vamling, L. and Theliander, H. (2016). Using 2D NMR to characterize the structure of the low and high molecular weight fractions of bio-oil obtained from LignoBoost™ kraft lignin depolymerized in subcritical water. Biomass and Bioenergy 95: 364–377. https://doi.org/10.1016/j.biombioe.2016.09.004

McClelland, D.J., Motagamwala, A.H., Li, Y., Rover, M.R., Wittrig, A.M., Wu, C., Buchanan, J.S., Brown, R.C., Ralph, J., Dumesic, J.A. and Huber, G.W. (2017). Functionality and molecular weight distribution of red oak lignin before and after pyrolysis and hydrogenation. Green Chem. 19: 1378–1389. https://doi.org/10.1039/c6gc03515a

Miller, J.E., Evans, L., Littlewolf, A. and Trudell, D.E. (1999). Batch microreactor studies of lignin and lignin model compound depolymerization by bases in alcohol solvents, Fuel. https://doi.org/10.1016/S0016-2361(99)00072-1

Nguyen, T.D.H., Maschietti, M., Åmand, L.E., Vamling, L., Olausson, L., Andersson, S.I. and Theliander, H. (2014a). The effect of temperature on the catalytic conversion of Kraft lignin using near-critical water. Bioresour. Technol. 170: 196–203. https://doi.org/10.1016/j.biortech.2014.06.051

Nguyen, T.D.H., Maschietti, M., Belkheiri, T., Åmand, L.E., Theliander, H., Vamling, L., Olausson, L. and Andersson, S.I. (2014b). Catalytic depolymerisation and conversion of Kraft lignin into liquid products using near-critical water. J. Supercrit. Fluids 86: 67–75. https://doi.org/10.1016/j.supflu.2013.11.022

Nielsen, J.B. (2016). Valorization of Lignin from Biorefineries for Fuels and Chemicals. Technical University of Denmark.

Okuda, K., Umetsu, M., Takami, S. and Adschiri, T. (2004). Disassembly of lignin and chemical recovery - Rapid depolymerization of lignin without char formation in water-phenol mixtures. Fuel Process. Technol. 85: 803–813. https://doi.org/10.1016/j.fuproc.2003.11.027

Orebom, A., Verendel, J.J. and Samec, J.S.M. (2018). High Yields of Bio Oils from Hydrothermal Processing of Thin Black Liquor without the Use of Catalysts or Capping Agents. ACS Omega 3: 6757–6763. https://doi.org/10.1021/acsomega.8b00854

Otromke, M., Shuttleworth, P.S., Sauer, J. and White, R.J. (2019a). Hydrothermal base catalysed treatment of Kraft lignin - time dependent analysis and a techno-economic evaluation for carbon fibre applications. Bioresour. Technol. Reports 6: 241–250. https://doi.org/10.1016/j.biteb.2019.03.008

Otromke, M., Shuttleworth, P.S., Sauer, J. and White, R.J. (2019b). Hydrothermal base catalysed treatment of Kraft Lignin for the preparation of a sustainable carbon fibre precursor. Bioresour. Technol. Reports 5: 251–260. https://doi.org/10.1016/j.biteb.2018.11.001

Pandey, M.P. and Kim, C.S. (2011). Lignin Depolymerization and Conversion: A Review of Thermochemical Methods. Chem. Eng. Technol. 34: 29–41. https://doi.org/10.1002/ceat.201000270

Parthasarathi, R., Romero, R.A., Redondo, A. and Gnanakaran, S. (2011). Theoretical study of the remarkably diverse linkages in lignin. J. Phys. Chem. Lett. 2: 2660–2666. https://doi.org/10.1021/jz201201q

Pedersen, T.H., Grigoras, I.F., Hoffmann, J., Toor, S.S., Daraban, I.M., Jensen, C.U., Iversen, S.B., Madsen, R.B., Glasius, M., Arturi, K.R., Nielsen, R.P., Søgaard, E.G. and Rosendahl, L.A. (2016). Continuous hydrothermal co-liquefaction of aspen wood and glycerol with water phase recirculation. Appl. Energy 162: 1034–1041. https://doi.org/10.1016/j.apenergy.2015.10.165

Pedersen, T.H., Jasiunas, L., Casamassima, L., Singh, S., Jensen, T. and Rosendahl, L.A. (2015). Synergetic hydrothermal co-liquefaction of crude glycerol and aspen wood. Energy Convers. Manag. 106: 886–891. https://doi.org/10.1016/j.enconman.2015.10.017

Rabinovich, M.L. (2010). Wood hydrolysis industry in the soviet union and Russia: A mini-review. Cellul. Chem. Technol. 44: 173–186.

Renders, T., Van Den Bosch, S., Koelewijn, S.F., Schutyser, W. and Sels, B.F. (2017). Lignin-first biomass fractionation: The advent of active stabilisation strategies. Energy Environ. Sci. 10: 1551–1557. https://doi.org/10.1039/c7ee01298e

Roberts, V.M., Stein, V., Reiner, T., Lemonidou, A., Li, X. and Lercher, J.A. (2011). Towards quantitative catalytic lignin depolymerization. Chem. - A Eur. J. 17: 5939–5948. https://doi.org/10.1002/chem.201002438

Rößiger, B., Röver, R., Unkelbach, G. and Pufky-Heinrich, D. (2017). Production of Bio-Phenols for Industrial Application: Scale-Up of the Base-Catalyzed Depolymerization of Lignin. Green Sustain. Chem. 07: 193–202. https://doi.org/10.4236/gsc.2017.73015

Saisu, M., Sato, T., Watanabe, M., Adschiri, T. and Arai, K. (2003). Conversion of lignin with supercritical water-phenol mixtures. Energy & Fuels 17: 922–928. https://doi.org/10.1021/ef0202844

Schutyser, W., Renders, T., Van Den Bosch, S., Koelewijn, S.F., Beckham, G.T. and Sels, B.F. (2018). Chemicals from lignin: An interplay of lignocellulose fractionation, depolymerisation, and upgrading. Chem. Soc. Rev. 47: 852–908. https://doi.org/10.1039/c7cs00566k

Sebhat, W. (2016). Valorisation de la lignine par catalyse hétérogène en condition sous-critique en milieux aqueux et eau/alcool. Université de Lyon.

Shuai, L., Amiri, M.T., Questell-Santiago, Y.M., Héroguel, F., Li, Y., Kim, H., Meilan, R., Chapple, C., Ralph, J. and Luterbacher, J.S. (2016a). Formaldehyde stabilization facilitates lignin monomer production during biomass depolymerization. Science (80-.). 354: 329 LP – 333. https://doi.org/10.1126/science.aaf7810

Shuai, L., Talebi Amiri, M. and Luterbacher, J.S. (2016b). The influence of interunit carbon–carbon linkages during lignin upgrading. Curr. Opin. Green Sustain. Chem. 2: 59–63. https://doi.org/10.1016/j.cogsc.2016.10.001

Thring, R.W. (1994). Alkaline degradation of ALCELL® lignin. Biomass and Bioenergy 7: 125–130. https://doi.org/10.1016/0961-9534(94)00051-T

Tomani, P. (2010). The lignoboost process. Cellul. Chem. Technol. 44: 53–58.

Wahyudiono, Sasaki, M. and Goto, M. (2008). Recovery of phenolic compounds through the decomposition of lignin in near and supercritical water. Chem. Eng. Process. Process Intensif. 47: 1609–1619. https://doi.org/10.1016/j.cep.2007.09.001

Wayman, M. and Lora, J.H. (1978). Aspen autohydrolysis: The effects of 2-naphthol and other aromatic compounds. Tappi 61: 55–57.

Wu, Y., Chen, Y. and Wu, K. (2014). Role of co-solvents in biomass conversion reactions using sub/supercritical water. In: Fang, Z., and Xu, C. (Charles) (Eds.). *Near-Critical and Supercritical Water and Their Applications for Biorefineries*. Springer, Dordrecht, pp. 69–98.

Yong, T.L.K. and Matsumura, Y. (2013). Kinetic analysis of lignin hydrothermal conversion in sub- and supercritical water. Ind. Eng. Chem. Res. 52: 5626–5639. https://doi.org/10.1021/ie400600x

Yong, T.L.K. and Matsumura, Y. (2012). Reaction kinetics of the lignin conversion in supercritical water. Ind. Eng. Chem. Res. 51: 11975–11988. https://doi.org/10.1021/ie300921d

Yoshikawa, T., Yagi, T., Shinohara, S., Fukunaga, T., Nakasaka, Y., Tago, T. and Masuda, T. (2013). Production of phenols from lignin via depolymerization and catalytic cracking. Fuel Process. Technol. 108: 69–75. https://doi.org/10.1016/j.fuproc.2012.05.003

Zakzeski, J., Bruijnincx, P.C.A., Jongerius, A.L. and Weckhuysen, B.M. (2010). The Catalytic Valorization of Lignin for the Production of Renewable Chemicals. Chem. Rev. 110: 3552–3599. https://doi.org/10.1021/cr900354u

Zhang, B., Huang, H.J. and Ramaswamy, S. (2008). Reaction kinetics of the hydrothermal treatment of lignin. Appl. Biochem. Biotechnol. 147: 119–131. https://doi.org/10.1007/s12010-007-8070-6